PROJECT REPORT FORM

PROJECT NO. 1102-9
COOPERATOR I.P.C.
REPORT NO. 1
DATE May 17, 1955
NOTE BOOK 605
PAGE 71 TO 92
SIGNED K. W. Hardacker

Copies to: Files
Van den Akker
Hardacker

K. W. Hardacker

SOME RESULTS OF A LOAD-ELONGATION INVESTIGATION WITH THE I.P.C. LOAD-ELONGATION APPARATUS

SPECIMEN LENGTH EFFECT

In his paper presented at the Symposium on Rheology of Cellulose Fibers and Sheets (ACS, September, 1954), Rance presented charts indicating that the load-elongation curves obtained for paper specimens identical in all respects but length differed substantially because of the difference in span length. In order to investigate the possibility of the existence of such a phenomenon, and to ascertain whether the effect is caused by jaw pull-out, it was suggested that a series of papers be tested on the I.P.C. load-elongation apparatus (DC 176). This equipment was chosen because it was thought the structure of its specimen clamps would eliminate clamping errors which might arise with conventional clamps. The papers were chosen to cover as wide a variety and to be as representative as possible while maintaining their number at a reasonable level. All are smooth surfaced. They are listed in Table I.

Specimens one inch in width were cut from these samples in both the machine and cross machine directions in lengths to provide initial testing spans of 2-1/2, 5, and 7-1/2 inches. An actual rate of travel of the lower clamp was chosen to provide a rate of elongation

which would be the same among the lengths. A rate of 0.15% per second was selected. Cutting and testing of the specimens was done in a room conditioned at 50% R.H., 73°F.

Load-elongation curves were obtained for five specimens of each sample at each length in both the machine and cross-machine directions. Data were read from each of these curves in the following manner. The load (in chart divisions) at which each specimen ruptured was noted. The minimum breaking load of a particular sample in a particular direction for its three span lengths was determined and measurements of percentage elongation made at this load from each of the fifteen curves in this group. Sixty per cent of this minimum breaking load was then calculated and measurements of elongation again made on the fifteen curves at this load. The percentage elongations at 100% and 60% of the minimum breaking load then provided a measure of the dependence of the load-strain curve on span length. Appropriate minimum breaking loads were chosen for each group. Table II lists the data as determined from the curves. A cursory examination of these data fails to reveal any definite trend.

COMMENTS ON THE LOAD-ELONGATION APPARATUS

All of the samples selected were satisfactorily tested on the load-elongation apparatus. A scale was attached to a fixed upright adjacent to the post supporting the limit switches. A pointer attached to the upper limit switch bracket then made it possible to set the upper

limit switch directly to provide the desired initial span length. This was found to be a great convenience when changing repeatedly from one span length to another.

The specimen clamps gripped the specimens securely when tightened by means of the knurled handles; but as this procedure eventually caused some discomfort to the hands, a hole was drilled crosswise through the end of each handle to permit entry of a rod. The resulting lever arrangement made clamping much easier. It also resulted, however, in an ability to apply too much clamping pressure to the specimen. A series of repeated specimen breaks at the clamps was traced to this cause: when the clamping pressure was lessened, the specimen ruptures occurred away from the clamps. Nevertheless, with this reduced clamping pressure the specimen was still gripped tightly enough to be transparentized in the clamping area. Evidence of desirable clamping characteristics are provided by stretched glassine specimens (one of which is attached to this page) which clearly show a sharp clamping line. No evidence of slippage in the clamps has been observed. In order to get the comparatively thick blotter stock in the lower clamp, it was necessary to spread the clamp very slightly each time.

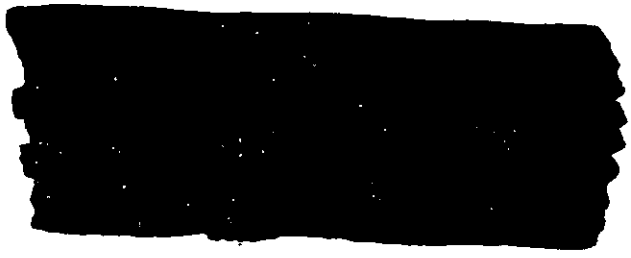

At the start of the present work, ruptures at the clamp were rather frequent. This was traced to improper adjustment of the clamping jig (used to align the specimen for clamping in the upper clamp). When this condition was corrected, the specimens were clamped in proper alignment and breaks at the clamp became rare. It was also observed that the toe of the load-elongation curve (the slowly rising portion at the very beginning of a curve--before the major rise commences) seemed to depend on the alignment of the specimen. When a specimen was deliberately misaligned, the toe was of appreciable extent; when clamped in good alignment, however, the toe was quite small. Occassionally a curve would be obtained in which the toe was nearly nonexistent, seemingly indicating near perfect alignment and clamping. (Clamping is included since any slippage from a poorly contacting area of a conventional clamp might well occur at initial loading.)

Hanging a fixed mass from the upper clamp after turning on the strain gage amplifier (operated through a Sorenson regulator) and allowing it to warm up produced slightly different indications on the recorder from one "turn on" to the next. During any one period of operation, however, (which might extend two or three days) the indication remained constant. The stability of the system under these conditions was very good: during the course of a series of tests at a particular amplifier gain setting, the bridge resistance balance control would need only occasional slight adjustment.

Specimen elongation is recorded by chart movement--the chart being driven from the elongation gear train. It was discovered that one could be assured of obtaining the initial portion of each load-elongation

curve if the backlash was removed from the recorder gear train before starting the specimen loading. This was accomplished with the following procedure.

1. After the previous specimen had ruptured, the Zero-Max was reversed to move the traveling bar upward. The recorder gear train system was not disturbed--it was left engaged, with the overrunning clutch preventing chart advance during the upward motion of the traveling bar.

2. When the traveling bar reached its starting point, it operated the upper limit switch, causing the motor to stop.

3. The specimen (already fastened in the upper clamp) was placed in position and the lower clamp tightened.

4. The push button which shorts out the limit switches was then depressed momentarily to cause the traveling bar to move still farther upward, but not far enough to operate the safety switch.

5. The Zero-Max reversing lever was then pulled forward, the recorder pen zero checked, and the shorting switch depressed and held down until the "Limit" neon extinguished.

TABLE I

LIST OF SAMPLES

Sample No.	Approx. BW, g/m^2	Description
1	42	Unbleached kraft
2	84	Unbleached kraft, wrapper
3	140	Unbleached kraft, liner
4	243	Standard blotter stock
5	47	Bleached sulfite, 100%
6	77	Bleached sulfite, 100%
7	76	Coating raw stock; 50% deinked fibers
8	47	Amber glassine, plasticized
9	52	Amber glassine, not plasticized
10	52	News, 79% groundwood
11	46	Rag, 100%
12	104	Rag, 100%
13	88	Coated, supercalendered (not sample 7 stock)
14	10.5	Condenser tissue, 0.0004 inch, kraft

TABLE II

SPECIMEN ELONGATIONS

Sample	Length, inches	Elongation, % 100% Minimum Breaking Load M.D.	Av.	X.D.	Av.	60% Minimum Breaking Load M.D.	Av.	X.D.	Av.
1	7.5	0.96	1.03	2.72	2.43	0.45	0.48	0.59	0.54
		1.04		2.35		0.48		0.53	
		0.99		2.40		0.48		0.53	
		1.01		2.29		0.48		0.53	
		1.15		2.40		0.51		0.53	
	5	0.96	1.14	2.40	2.59	0.48	0.54	0.52	0.54
		1.16		2.44		0.60		0.52	
		1.04		2.84		0.52		0.52	
		1.16		2.92		0.56		0.60	
		1.40		2.36		0.56		0.52	
	2.5	1.04	1.14	2.64	2.74	0.48	0.50	0.56	0.54
		1.04		3.36		0.48		0.56	
		1.12		3.00		0.48		0.56	
		1.12		2.36		0.48		0.52	
		1.36		2.36		0.56		0.52	
2	7.5	1.12	1.17	1.70	1.70	0.48	0.51	0.58	0.58
		1.06		1.66		0.48		0.58	
		1.22		1.70		0.54		0.58	
		1.28		1.70		0.54		0.58	
		--		1.76		--		0.58	
	5	1.12	1.28	1.74	1.72	0.50	0.53	0.56	0.56
		1.28		1.80		0.52		0.58	
		1.58		1.88		0.62		0.58	
		1.28		1.58		0.54		0.54	
		1.14		1.60		0.48		0.54	
	2.5	1.56	1.22	1.40	1.81	0.64	0.54	0.52	0.58
		1.12		1.68		0.52		0.56	
		1.20		1.80		0.52		0.60	
		1.08		2.00		0.48		0.60	
		1.16		2.16		0.52		0.64	

TABLE II (Continued)

Sample	Length, inches	Elongation, % 100% Minimum Breaking Load M.D.	Av.	X.D.	Av.	60% Minimum Breaking Load M.D.	Av.	X.D.	Av.
3	7.5	2.13	2.17	3.31	3.31	0.77	0.82	0.80	0.81
		2.03		3.31		0.80		0.80	
		2.00		3.20		0.80		0.80	
		2.29		3.36		0.85		0.80	
		2.35		3.41		0.88		0.85	
	5	2.14	2.21	3.72	3.61	0.82	0.84	0.84	0.82
		2.20		3.72		0.84		0.84	
		2.12		3.68		0.82		0.84	
		2.22		3.52		0.84		0.80	
		2.38		3.40		0.88		0.80	
	2.5	2.40	2.53	3.20	3.07	0.92	0.96	0.80	0.78
		2.52		3.12		0.96		0.80	
		2.56		2.92		0.96		0.76	
		2.56		3.04		1.00		0.76	
		2.64		3.08		1.00		0.80	
4	7.5	1.05	0.95	1.71	1.77	0.41	0.40	0.52	0.52
		0.99		1.84		0.40		0.52	
		0.93		1.81		0.39		0.53	
		0.91		1.76		0.39		0.53	
		0.88		1.76		0.39		0.52	
	5	0.86	0.90	1.92	1.83	0.40	0.40	0.54	0.54
		0.94		2.06		0.40		0.56	
		0.92		1.74		0.40		0.54	
		0.90		1.66		0.40		0.52	
		0.86		1.76		0.38		0.54	
	2.5	1.16	1.03	2.52	2.44	0.44	0.41	0.60	0.59
		1.08		2.40		0.44		0.60	
		0.96		2.52		0.40		0.60	
		1.00		2.52		0.40		0.60	
		0.96		2.24		0.40		0.56	
5	7.5	1.11	1.11	1.45	1.52	0.45	0.46	0.47	0.48
		1.20		1.52		0.48		0.48	
		1.04		1.53		0.44		0.49	
		1.07		1.51		0.45		0.47	
		1.15		1.53		0.47		0.48	

TABLE II (Continued)

Sample	Length, inches	Elongation, % 100% Minimum Breaking Load M.D.	Av.	X.D.	Av.	60% Minimum Breaking Load M.D.	Av.	X.D.	Av.
	5	1.02	1.04	1.62	1.64	0.44	0.44	0.46	0.48
		1.08		1.56		0.44		0.48	
		1.02		1.68		0.44		0.48	
		1.04		1.60		0.44		0.46	
		1.04		1.76		0.44		0.52	
	2.5	1.04	1.08	1.20	1.38	0.44	0.46	0.40	0.45
		1.08		1.36		0.48		0.44	
		1.12		1.32		0.48		0.44	
		1.02		1.52		0.44		0.48	
		1.12		1.52		0.48		0.48	
6	7.5	1.20	1.21	1.84	1.83	0.48	0.48	0.51	0.51
		1.23		1.81		0.48		0.51	
		1.20		1.92		0.48		0.51	
		1.20		1.76		0.48		0.51	
		--		1.81		--		0.51	
	5	1.00	1.08	1.82	1.78	0.40	0.43	0.48	0.47
		1.12		1.86		0.44		0.48	
		1.12		1.86		0.44		0.48	
		1.04		1.66		0.44		0.46	
		1.10		1.68		0.44		0.46	
	2.5	1.12	1.14	1.80	1.62	0.48	0.46	0.48	0.48
		1.16		1.68		0.48		0.48	
		1.16		1.64		0.48		0.48	
		1.16		1.52		0.44		0.48	
		1.12		1.48		0.44		0.48	
7	7.5	0.88	0.88	1.60	1.75	0.40	0.40	0.48	0.49
		1.01		1.79		0.47		0.48	
		0.85		1.81		0.40		0.51	
		0.83		1.87		0.37		0.51	
		0.83		1.68		0.37		0.48	

TABLE II (Continued)

Sample	Length, inches	Elongation, % 100% Minimum Breaking Load M.D.	Av.	X.D.	Av.	60% Minimum Breaking Load M.D.	Av.	X.D.	Av.
	5	1.02	0.92	1.72	1.54	0.42	0.40	0.48	0.46
		0.92		1.64		0.40		0.48	
		0.94		1.42		0.40		0.44	
		0.82		1.44		0.38		0.44	
		0.88		1.46		0.40		0.44	
	2.5	0.92	0.93	1.36	1.36	0.40	0.41	0.48	0.45
		0.88		1.36		0.40		0.44	
		0.88		1.36		0.40		0.44	
		0.96		1.32		0.40		0.44	
		1.00		1.40		0.44		0.44	
8	7.5	1.15	1.13	3.25	3.14	0.48	0.49	0.48	0.49
		1.23		3.20		0.51		0.51	
		1.15		3.36		0.51		0.51	
		1.09		3.09		0.48		0.48	
		1.04		2.80		0.45		0.48	
	5	1.00	1.05	2.64	2.76	0.44	0.45	0.44	0.46
		1.00		2.64		0.44		0.46	
		1.02		2.84		0.44		0.46	
		1.08		2.88		0.46		0.48	
		1.14		2.78		0.46		0.46	
	2.5	1.04	1.06	1.80	2.34	0.48	0.46	0.40	0.46
		1.12		2.56		0.48		0.44	
		1.04		2.60		0.44		0.48	
		0.96		2.40		0.44		0.48	
		1.12		2.36		0.48		0.48	
9	7.5	1.01	0.99	3.28	3.35	0.48	0.48	0.51	0.52
		0.99		3.41		0.48		0.53	
		0.99		3.44		0.48		0.51	
		0.93		3.25		0.48		0.51	
		1.04		3.39		0.48		0.53	
	5	1.10	1.08	3.54	3.54	0.48	0.47	0.52	0.52
		1.10		3.54		0.48		0.52	
		1.06		3.64		0.46		0.54	
		1.04		3.54		0.46		0.50	
		1.10		3.42		0.48		0.50	

TABLE II (Continued)

Sample	Length, inches	Elongation, % 100% Minimum Breaking Load M.D.	Av.	X.D.	Av.	60% Minimum Breaking Load M.D.	Av.	X.D.	Av.
	2.5	1.04	1.06	3.44	3.36	0.48	0.48	0.56	0.54
		1.12		3.40		0.48		0.56	
		1.08		3.20		0.48		0.52	
		1.04		3.36		0.48		0.52	
		1.04		3.40		0.48		0.52	
10	7.5	0.67	0.69	0.93	0.86	0.35	0.35	0.45	0.43
		0.76		0.88		0.35		0.44	
		0.68		0.84		0.37		0.43	
		0.65		0.81		0.35		0.41	
		0.67		0.84		0.35		0.43	
	5	0.66	0.67	1.06	1.02	0.36	0.36	0.48	0.48
		0.68		1.02		0.36		0.48	
		0.68		1.02		0.36		0.48	
		0.66		1.00		0.36		0.46	
		0.68		0.98		0.36		0.48	
	2.5	0.72	0.75	1.04	0.98	0.40	0.42	0.48	0.46
		0.72		1.04		0.40		0.48	
		0.72		1.00		0.36		0.48	
		0.72		0.96		0.40		0.48	
		0.88		0.88		0.56		0.40	
11	7.5	1.59	1.54	3.12	3.27	0.48	0.49	0.59	0.62
		1.49		3.17		0.47		0.59	
		1.47		3.31		0.47		0.64	
		1.61		3.23		0.56		0.64	
		1.52		3.52		0.48		0.64	
	5	1.48	1.39	3.14	2.98	0.46	0.45	0.60	0.59
		1.34		2.84		0.44		0.56	
		1.38		2.64		0.46		0.56	
		1.40		3.04		0.46		0.60	
		1.34		3.06		0.44		0.62	
	2.5	1.44	1.44	2.16	2.53	0.48	0.50	0.56	0.57
		1.44		2.16		0.48		0.56	
		1.44		2.64		0.48		0.56	
		1.32		2.80		0.48		0.60	
		1.56		2.88		0.56		0.56	

TABLE II (Continued)

Sample	Length, inches	Elongation, % 100% Minimum Breaking Load M.D.	Av.	X.D.	Av.	60% Minimum Breaking Load M.D.	Av.	X.D.	Av.
12	7.5	2.77	2.81	5.87	5.92	0.77	0.79	1.25	1.25
		2.80		5.73		0.80		1.23	
		2.83		6.08		0.80		1.28	
		2.80		6.05		0.80		1.25	
		2.83		5.89		0.80		1.25	
	5	2.96	3.04	6.04	6.18	0.82	0.84	1.26	1.28
		3.08		6.44		0.84		1.30	
		3.10		6.72		0.84		1.38	
		3.02		5.74		0.84		1.20	
		3.04		5.94		0.84		1.26	
	2.5	3.28	3.22	5.28	5.40	0.88	0.88	1.20	1.19
		3.20		5.56		0.88		1.20	
		3.12		5.64		0.88		1.20	
		3.48		5.12		0.88		1.16	
		3.04		5.40		0.88		1.20	
13	7.5	0.83	0.79	1.57	1.55	0.37	0.36	0.43	0.43
		0.85		1.49		0.37		0.43	
		0.77		1.57		0.37		0.43	
		0.77		1.55		0.35		0.43	
		0.75		1.55		0.35		0.43	
	5	0.76	0.74	1.44	1.54	0.36	0.35	0.40	0.40
		0.72		1.46		0.34		0.40	
		0.76		1.54		0.36		0.40	
		0.72		1.60		0.34		0.40	
		0.72		1.64		0.34		0.42	
	2.5	0.76	0.74	1.48	1.46	0.36	0.36	0.40	0.40
		0.76		1.44		0.36		0.40	
		0.72		1.44		0.36		0.40	
		0.72		1.44		0.36		0.40	
		0.72		1.48		0.36		0.40	
14	7.5	1.07	1.06	1.12	1.25	0.45	0.45	0.45	0.45
		1.04		1.23		0.45		0.43	
		1.07		1.39		0.45		0.48	
		1.04		--		0.45		--	
		1.09		--		0.45		--	

TABLE II (Continued)

Sample	Length, inches	Elongation, % 100% Minimum Breaking Load M.D.	Av.	X.D.	Av.	60% Minimum Breaking Load M.D.	Av.	X.D.	Av.
	5	1.04	1.05	1.08	1.14	0.44	0.46	0.38	0.41
		1.16		1.24		0.56		0.44	
		1.04		1.12		0.44		0.40	
		1.02		1.20		0.44		0.44	
		1.00		1.04		0.44		0.40	
	2.5	1.04	1.03	1.16	1.09	0.44	0.46	0.40	0.40
		1.04		1.12		0.52		0.40	
		1.08		1.00		0.48		0.40	
		1.00		1.16		0.44		0.40	
		1.00		1.00		0.44		0.40	

PROJECT REPORT FORM

Copies to: Files
Lathrop
Van den Akker
Reading Copy

PROJECT NO. 1102-9
COOPERATOR
REPORT NO. 2
DATE January 3, 1961
NOTE BOOK
PAGE TO
SIGNED A. L. Lathrop

ANAMORPHIC TELESCOPE REPORT

In graphic arts work there is sometimes a need to make a photocopy that will produce a stretched photographic image. In particular it may be desired to copy a square figure as a rectangle. This result is most easily accomplished by placing in front of the copy camera an opera glass or galilean telescope that is made with cylindrical objective and ocular lenses with parallel axes. If the telescope is designed to form a slightly magnified image that is nearly coplanar with the object being viewed, the desired result will be achieved.

Laboratory tests show that magnifications (or "stretch ratios") of unity up to 4/3 are possible using simple ophthalmic quality lenses. At these lower magnifications there was some evidence of lateral chromatism. A test at a magnification of 2.0 with simple lenses suggests that, at these higher magnifications, curvature of field is also a problem.

The theory of such telescopes is presented here. Figure 1 shows a diagram of such a telescope. In the figure, F_1 denotes the focal length of the positive objective lens and F_2 that of the negative ocular. The camera lens will, of course, be placed adjacent to the ocular. The object distances are denoted as S with the appropriate subscript, and the image distances as S'. The separation between the lenses, D, is positive as shown. The object and image distances follow the common sign convention, and are positive or negative as indicated in the figure for the case shown. The object and image heights are y and y' respectively.

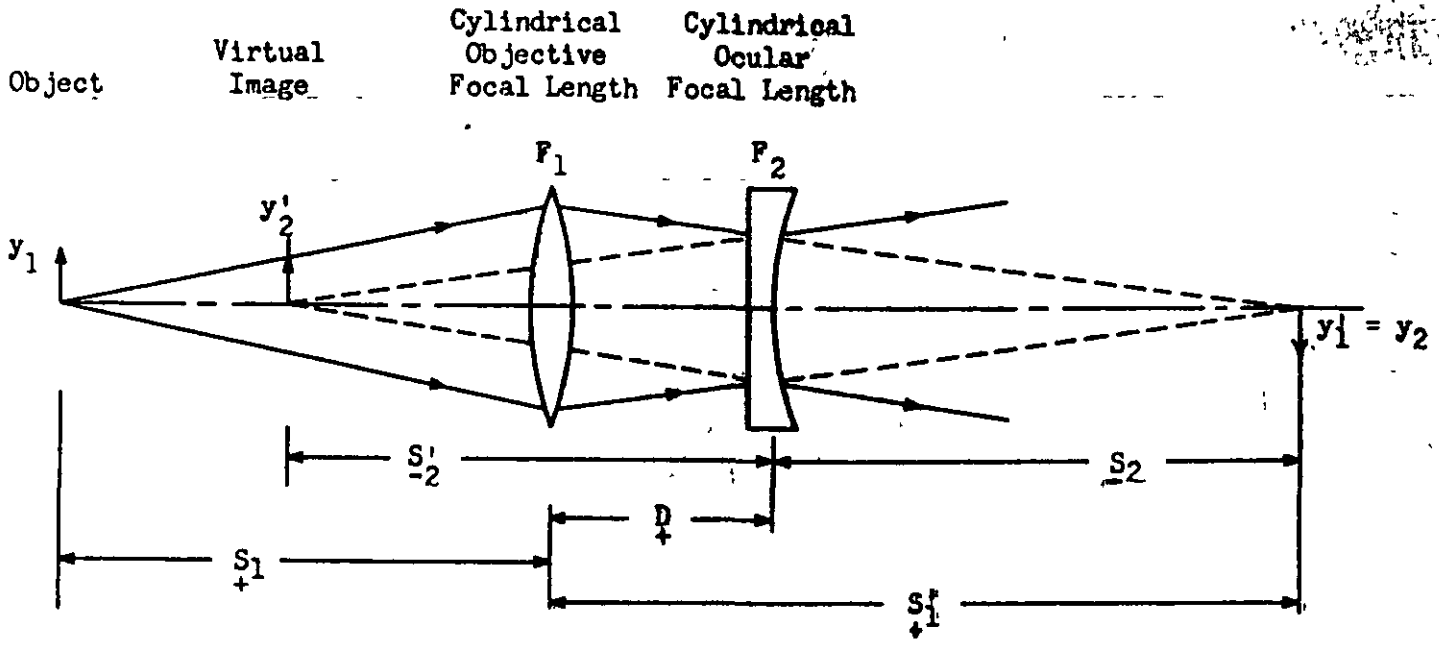

The anamorphic telescope. The axes of the cylindrical lenses are perpendicular to the plane of the paper.

Figure 1

First the conditions will be determined under which the object and image are coplanar. The lens equation that describes the behavior of image points with spherical lenses, holds as well for image "lines" with cylindrical lenses.

I. Solve for S_2'

1 (a) $$S_1' = (S_1F_1)/(S_1-F_1)$$

1 (b) $$S_2 = D - S_1'$$

1 (c) $$S_2' = (S_2F_2)/(S_2-F_2)$$

$$= \frac{F_2[D(S_1-F_1)-S_1F_1]}{D(S_1-F_1)-S_1F_1-F_2(S_1-F_1)}$$

The condition for a coplanar object and image is:

1 (d) $\qquad S_2' = -S_1 - D$

Substituting 1 (d) in 1 (c) gives the desired relationship:

1 (e) $\qquad AD^2 + BD + C = 0$

Where $A = S_1 - F_1$

$B = S_1^2 - 2S_1F_1$

$C = -S_1^2 (F_1 + F_2)$

In practice one will find it most convenient to keep the camera lens, the ocular, and the object fixed. Then the telescope will be focussed by varying the position of the objective lens. For this reason it is desirable to put Equation 1 (e) in a different form in which $S_1 + D$ is taken as a constant unit length.

Define the new dimensionless variables:

$d = D/(S_1 + D) \qquad f_2 = F_2/(S_1 + D)$

$f_1 = F_1/(S_1 + D) \qquad s_1 = S_1/(S_1 + D) = 1-d$

If the telescope objective lens is moved, d and s_1 change but the other variables defined here do not. Then the condition for a coplanar object and image becomes:

1 (f) $\qquad ad^2 + bd + c = 0$

Where $a = 1 + f_2$

$b = -1 - 2f_2$

$c = f_1 + f_2$

Figure 2 shows the plot of d (f_1) for different values of f_2.

The second important step will be to determine the angular magnification of the telescope as it will be seen from the position of the ocular. The camera lens is, of course, placed adjacent to the ocular; so the angular magnification as derived here is equal to the lateral magnification caused by the telescope on the film plane of the camera.

2 (a) Angular Magnification, $M = [y_2'/-S_2']/[y_1/(S_1 + D)]$

But in the dimensionless variables, $S_1 + D = 1$

and $y_2/y_1 = -s_1'/s_1$

$y_2'/y_2 = -s_2'/s_2 = s_2'/(s_1' - d)$

Substituting:

2 (b) $M = s_1'/[(s_1' - d)(1 - d)]$

But from Equation 1 (a):

$s_1' = s_1 f_1/(s_1 - f_1) = (1 - d)f_1/(1 - d - f_1)$

2 (c) $M = f_1/(f_1 - d + d^2)$

And for small values of d/f_1 and d:

2 (d) $M \simeq 1 + d/f_1$ ----

So, as a first approximation, the magnification depends on the ratio D/F_1 and not on the object distance.

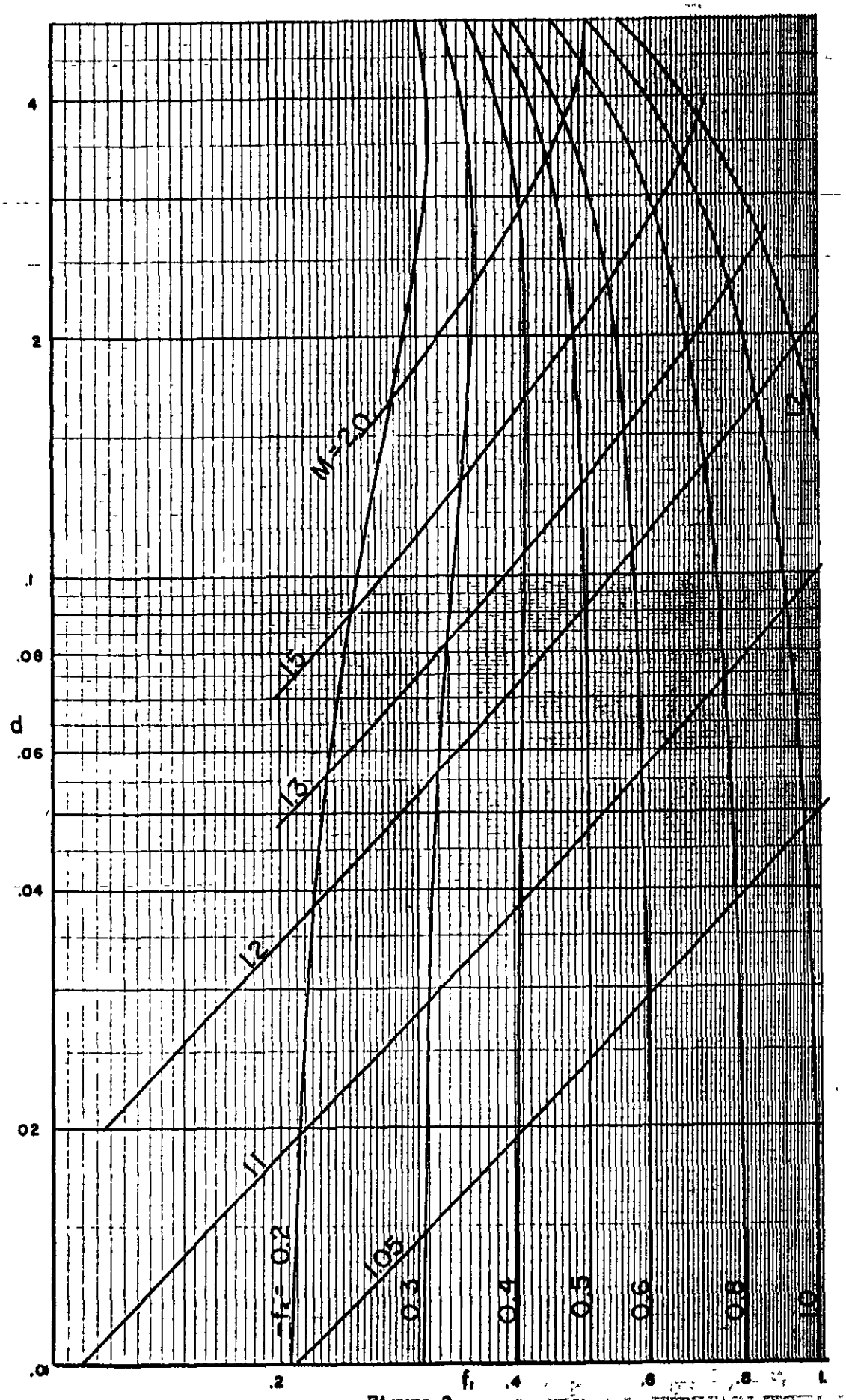
4
2
.1
.08
.06
.04
.02
.01
d
.2
.4
.6
.8
1
f_1
M=2.0
1.5
1.3
1.2
1.1
1.05
f_2= 0.2
0.3
0.4
0.5
0.6
0.8
1.0

Figure 2

It should be observed that the magnification is not dependent on the focal length of the ocular, F_2. The ocular is important only as a means of controlling the position of the image formed by the telescope. Equation 2 (c) then gives the correct value of the magnification regardless of whether or not the object and image are coplanar. Equation 2 (c) is also plotted in Figure 2. It will be recognized that this magnification occurs in only one direction, the direction in the object plane that is perpendicular to the lens axes. Hence, a magnification of 1.2 times means that the image is "stretched" by 20%.

The magnification formula 2 (c) is also the basis of a simple explanation of the lateral chromatism that is observed. The magnification of the telescope depends on the focal length f_1, and the separation distance, d. The focal length f_1, varies in turn with the index of refraction of the glass in the objective lens at different wavelengths, but d does not. From Equation 2 (c) it follows:

$$2\ (e) \qquad M/(M-1) = f_1/(d - d^2)$$

The focal length of a lens can be shown to vary with small increments of the index of refraction dn:

$$2\ (f) \qquad df_1 = -f_1\ dn/(n-1)$$

Differentiate 2 (e), and substitute 2 (f). The desired result follows:

$$2\ (g) \qquad dM = dn\ M(M-1)/(n-1)$$

It is important to observe that the amount of lateral chromatism depends only on the magnification and not on the particular combination of f_1 and d that causes that magnification. Also the amount of "spreading" of an image line can be calculated if the values of n are known at the ends of the spectral band of light

used. Furthermore, this lateral chromatism should be effectively eliminated if the objective lens were an achromatic doublet.

Figure 2, then, shows much of the information that is needed to make practical design determinations for an anamorphic telescope. It should be noted in particular that when $f_1 = 0.4$ to 0.5, the lines of constant f_2 are approximately straight vertical lines. The indication is plain. It should be possible in this case to change the magnification by moving the objective lens over a considerable range and still keep the object and image nearly coplanar. This possibility should be pursued further, and so the question of depth of field of the camera is now considered.

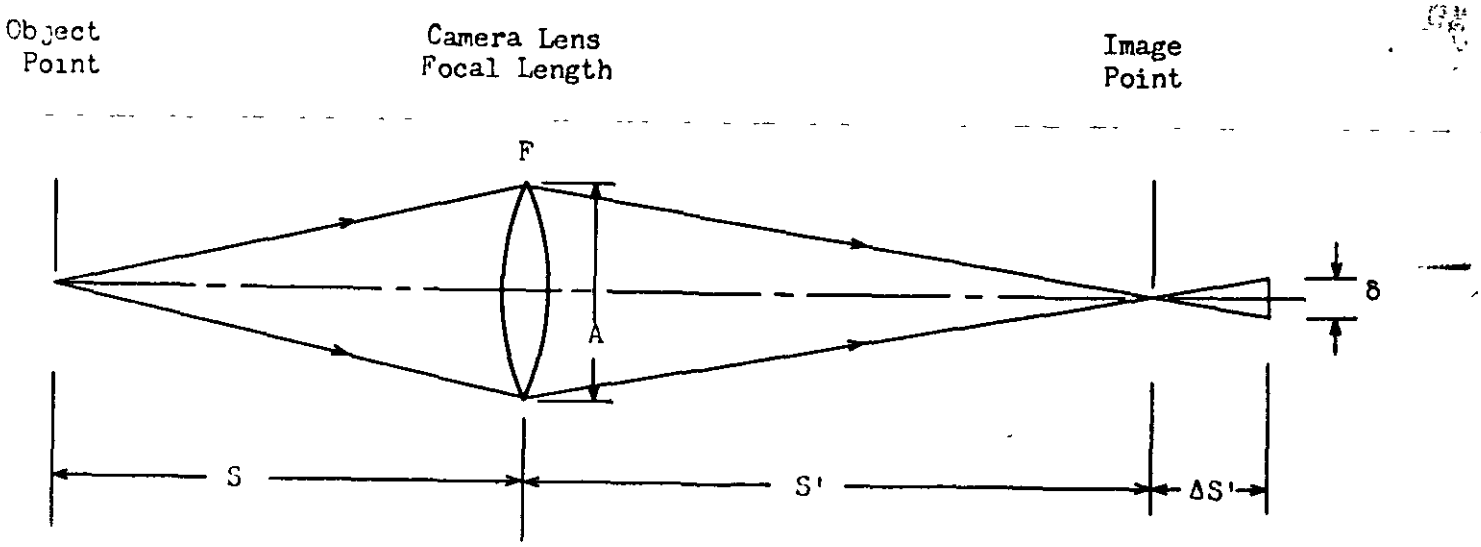

Depth of field of the copy camera lens.

Figure 3

The problem of the depth of field of the camera is considered with reference to Figure 3. The focal length of the lens is F. The object and image distances are S and S'. If the image is observed at a short distance $\Delta S'$ from the plane of best focus, the image "point" will then appear to be a circular disc of light of diameter δ. In ordinary photographic practice δ will be a small fraction of the focal length. According to the Kodak Reference Handbook, a rule for critical focus would be: $F/\delta \geq 1{,}000$ to $1{,}700$. This rule is intended for general pictorial photography with lenses of "normal" focal length. For copy work the rule will be rewritten:

$$3\,(a) \qquad S'/\delta = L$$

Where L is the large number of 1,000 to 1,700. (If one uses a copy camera lens with an unusually long focal length and narrow field of view, still larger values of L may be desired.)

From the similar triangles in Figure 3 it follows that:

$$3\,(b) \qquad \delta/S' = A/S'$$

If this equation is combined with 3 (a) and the simple lens equation, Equation 1 (a), it can then be shown that:

$$3\,(c) \qquad \Delta S/S = \underline{f}\,(1 + M)/[ML \pm \underline{f}\,(1 + M)^2]$$

Where:

ΔS is the change in the object distance corresponding to the change in image distance from S' to S' + $\Delta S'$.

$\underline{f}$ is the relative aperture, F/A, as marked on the lens barrel.

M is the magnitude (positive) of lateral magnification, S'/S.

Referring back to Figure 1, let $S_1 + D$ be equal to S in Figure 3, because both distances are the distance between the camera lens and a real object point. Now suppose that the anamorphic telescope does not have a coplanar object and image. That is, $S_1 + D \neq S_2'$, but instead the two distances differ by amount ΔS. If ΔS is less than the value given by Equation 3 (c), the depth of field of the camera will be sufficient to simultaneously focus the two planes.

Numerical examples will now show that this depth of field can be quite considerable. Let L = 1,500, and suppose the camera is set to record at unit magnification at f/90. Even at this small aperture the diffraction effects of the small lens aperture will be practically insignificant in ordinary graphic arts work. The indicated calculation shows that $\Delta S/S$ = .159 and .097; that is, the coplanar condition can be off by 16% on the far side and 10% on the near side. One's individual practice may indicate to him the need to use a larger lens stop or a different number L, but in any case a considerable margin in focus can clearly be tolerated.

Even if f/32 were used instead of f/90 the corresponding tolerances in the sample problem given above would still be as high as about 4.7% and 4%.

Figures 4, 5, and 6 show that the numerical values given for the allowable depth of field are quite adequate in many situations. In each of these graphs, $s_2' = S_2'/(S_1 + D)$ is plotted against d, with lines of constant magnification drawn in. Figure 4 shows the behavior of a telescope for which $F_2 = -F_1$. It is apparent that magnification ratios up to about 1.5 are quite feasible if the object distance is adjusted to put f_1 anywhere in the range 0.41 to 0.5, assuming the coplanar condition can be off 16% and 10% as mentioned in the previous paragraph.

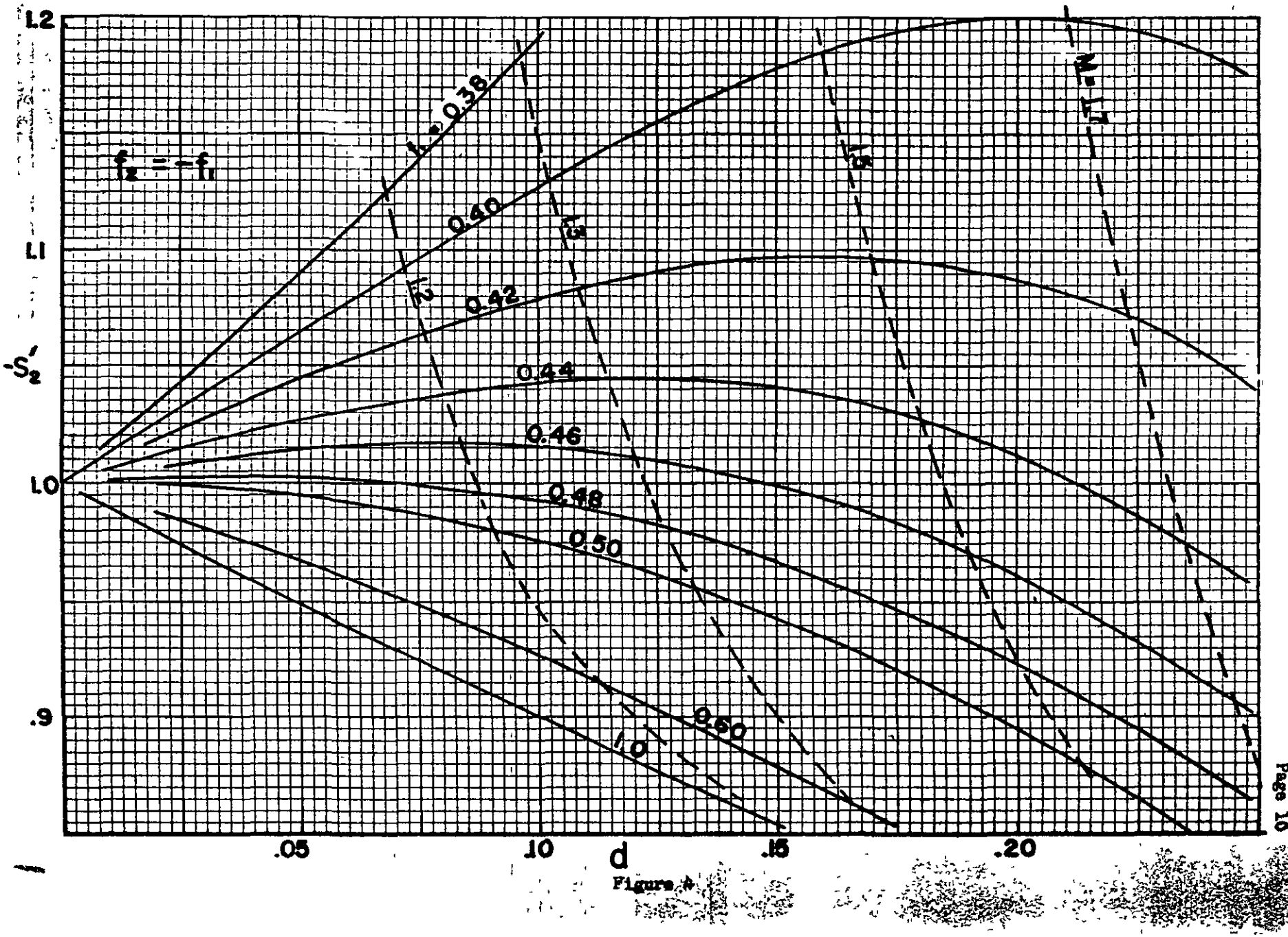
1.2
1.1
1.0
.9
S_2'
$f_2 = -f_1$
$L = 0.38$
0.40
0.42
0.44
0.46
0.48
0.50
0.60
1.0
F_2
F_3
F_4
F_5
.05
.10
.15
.20
d

Figure 4

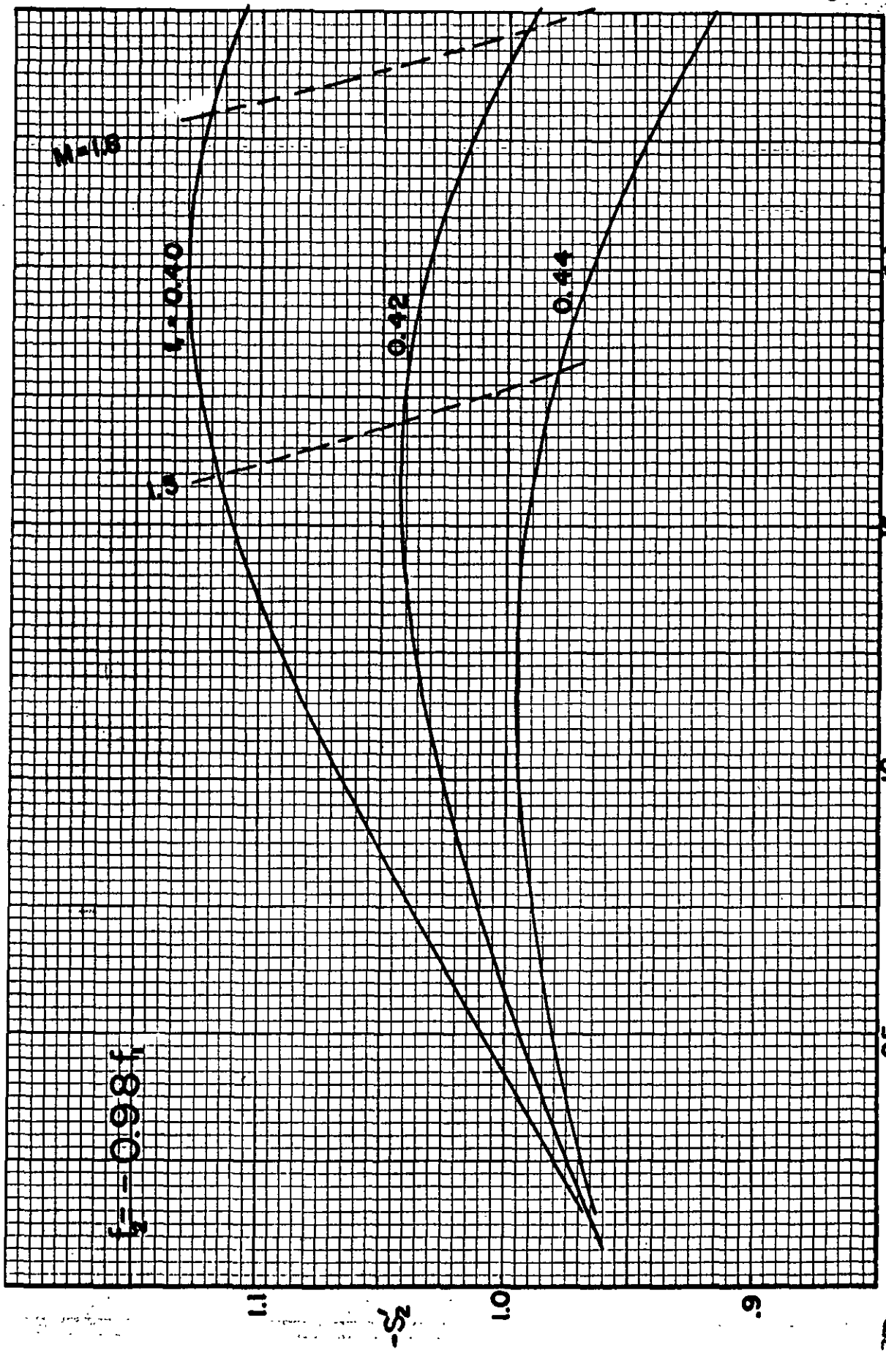

Figure 5

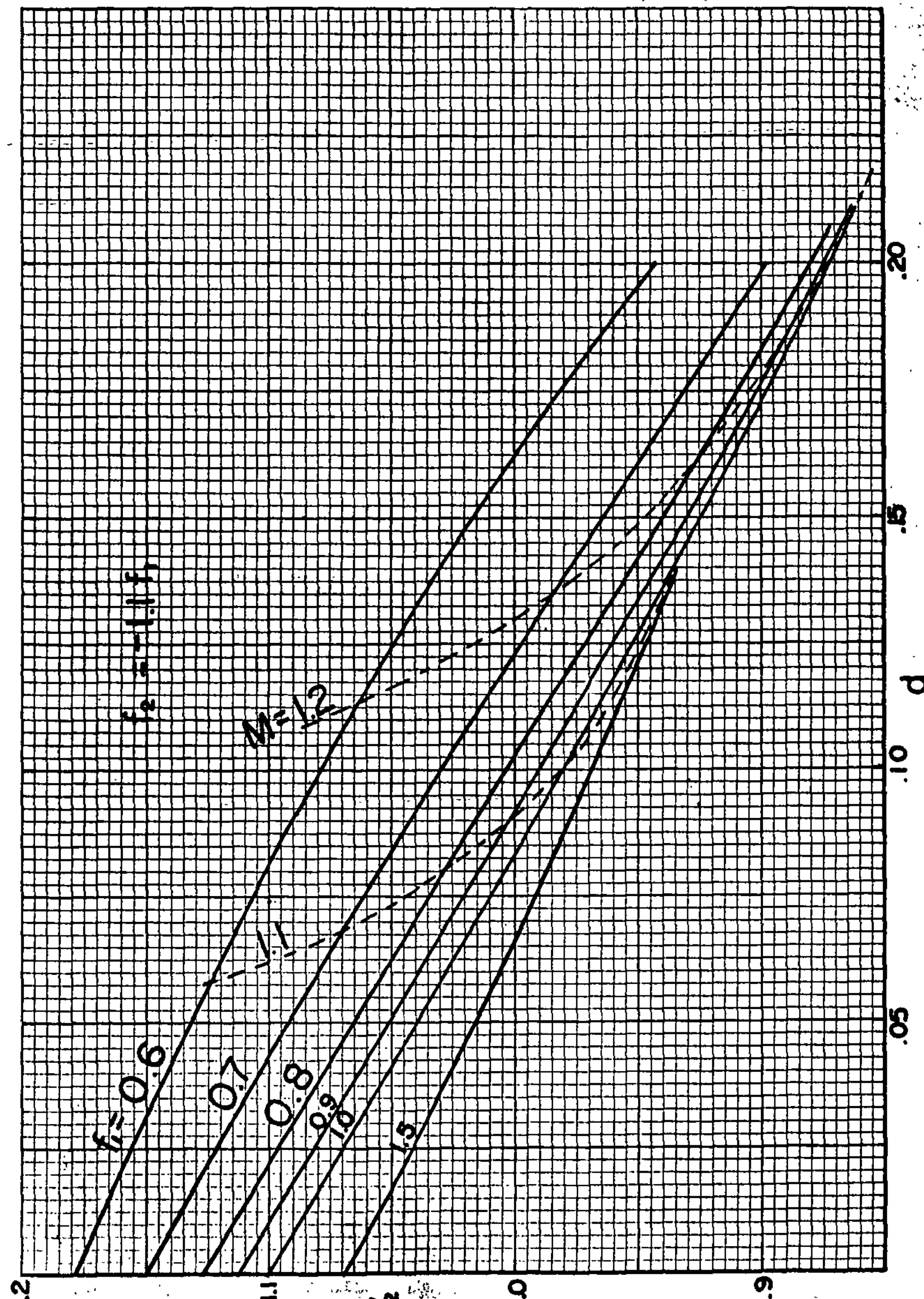

Figure 6

Figure 5 shows that, if the telescope is redesigned so that $F_2 = -0.98F_1$, much less depth of field is necessary if the object distance can be kept more nearly fixed so that $f_1 = 0.42$ to 0.44. Magnification values up to about 2.0 should be possible in this case.

From an inspection of Figures 4 and 5, it is apparent that the big advantage in using values of f_1 of about 0.4 to 0.5 lies in the fact that a particularly wide range of magnifying powers is permitted. This fact is directly dependent on the existence of a minimum value of S_2' at conveniently small values of d, when f_1 lies in this range. The nature of the function $s_2'(d)$ is considered here in more detail. The results that are summarized may be useful in solving detailed design problems for a telescope.

Equation 1 (c) can be rewritten in dimensionless co-ordinates:

$$4\,(a) \qquad s_2' = f_2\,(d - d^2 - f_1)/[d - d^2 - f_1 - f_2(1 - d - f_1)]$$

For constant f_1, an extreme value of s_2' exists when:

$$4\,(b) \qquad d = d_{max} = 1 - 2f_1$$

and at this value of d:

$$4\,(c) \qquad s_2'(d) = s_2'(d_{max}) = f_2\,(4f_1 - 1)/(4f_1 - 1 + f_2)$$

also when d = 0:

$$4\,(d) \qquad s_2'(d) = s_2'(0) = f_1 f_2/(f_1 + f_2 - f_1 f_2)$$

Now define d_o as that nonvanishing value of d for which $s_2'(d) = s_2'(0)$.

$$4\,(e) \qquad d_o = (1 - 2f_1)/(1 - f_1)$$

And the corresponding values of magnification are:

$$4\,(f) \qquad M\,(d_{max}) = 1/(4\,f_1 - 1)$$

$$4\,(g) \qquad M\,(d_o) = [(1 - f_1)/f_1]^2$$

These equations can be checked for a few special cases on the graphs in Figures 4 and 5. Equations 4 (b), 4 (e), 4 (f), and 4 (g) are plotted in Figure 7.

The use of these equations is now shown. One will first observe the depth of field of his copy camera for the particular object distance and minimum relative aperture that he plans to use. The object distance for perfect focus is taken as unity. The minimum and maximum distances of good focus are respectively $s_2'\,(0)$ and $s_2'\,(d_{max})$. Solving Equations 4 (c) and 4 (d), one can find appropriate values of f_1 and f_2. The telescope so designed will permit any magnification from unity to $M\,(d_o)$. If these limits of good focus had been taken to be -0.95 and -1.05 units, we observe from Figure 5 that the approximate solution is $f_1 = 0.42$, $f_2 = -0.98f_1$.

A telescope can be designed so that the coplanar object and image would be at a principal focus of both the objective and ocular. In that case the light in the telescope is collimated, $F_2 = -S_1 - D$, and the magnification is obviously $M = -F_2/F_1$. If the magnification is to be about 1.1, then f_1 is about 0.9. Figure 6 shows the focus conditions for this telescope. Ordinarily, this kind of design with larger values of f_1 may not be desired. A longer telescope is required. However, if only small magnifications are required ($M < 1.15$) there may be an advantage in having the magnification less sensitive to small changes in d.

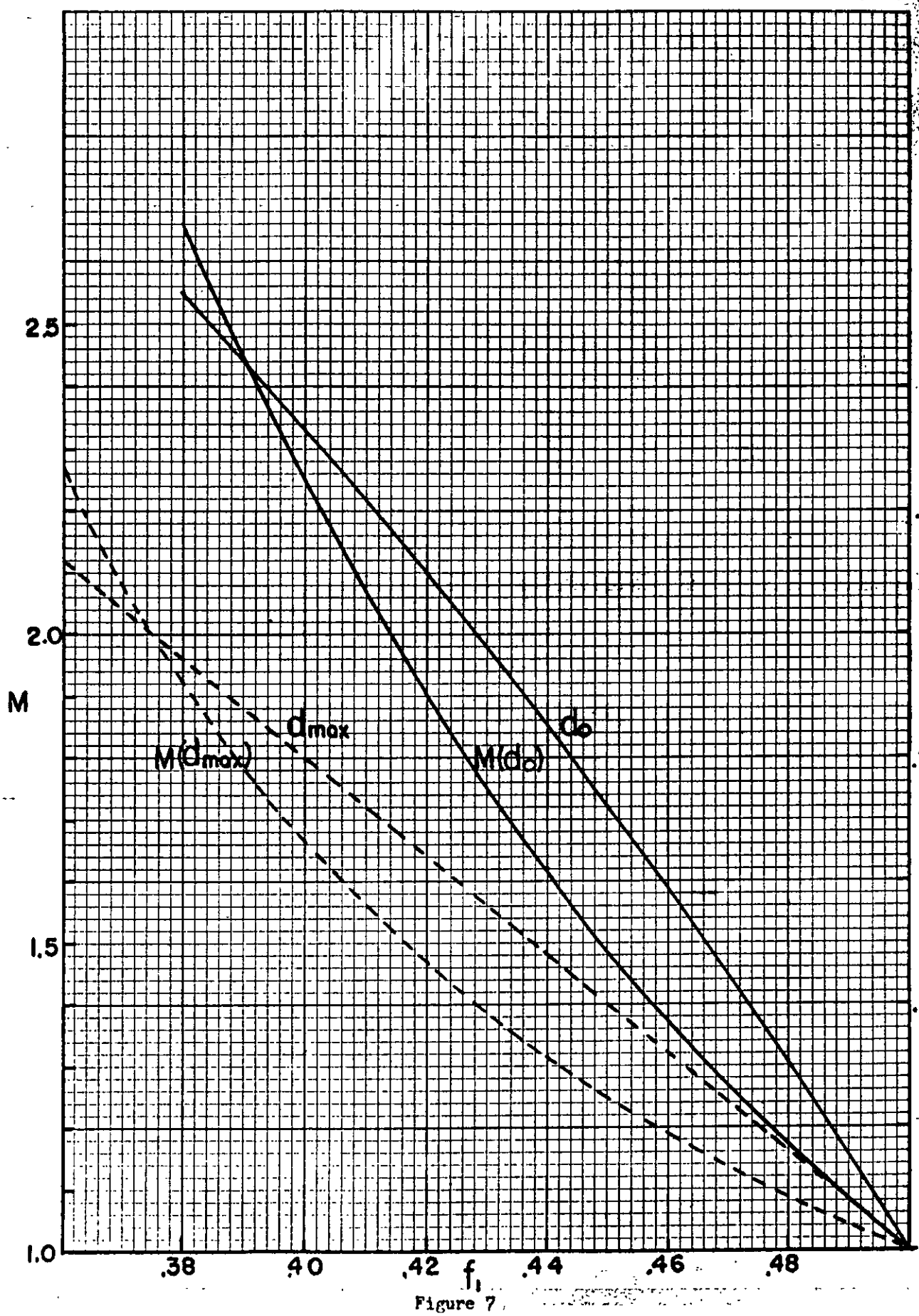

Figure 7

It will ordinarily not be desirable to design a telescope to operate with values of f_1 less than about 0.4. There is, however, one situation that may make this desirable. Suppose one wanted to have a telescope magnification of about 2.0 or greater. This ordinarily demands a large value of d, and this in turn may lead to a reduced useful angle of view.

There is a possible way out of this trouble. As Figure 2 shows, one can get a greater magnification at smaller values of d by using smaller values of f_1. That is, one can use a shorter telescope if both the objective and ocular are "stronger" lenses.

For example, Figure 2 shows that the coplanar condition is approximately satisfied when $f_1 = 0.28$ and $f_2 = -0.2 = -0.714f_1$. This corresponds approximately to M = 2.0 and d = 0.17. To investigate the possibility of making such a telescope, another plot similar to Figures 4, 5, and 6 is shown. Figure 8 shows a family of curves for the condition $f_2 = -0.714f_1$. These curves show that magnifications of 2.0 and greater are quite possible as predicted. However, a price must be paid. It is not possible to change the magnification very much without also changing the object distance (i.e. without changing f_1).

This does not appear to be the type of design that will ordinarily be desired, but the sample problem does show the possibilities of working at smaller values of f_1.

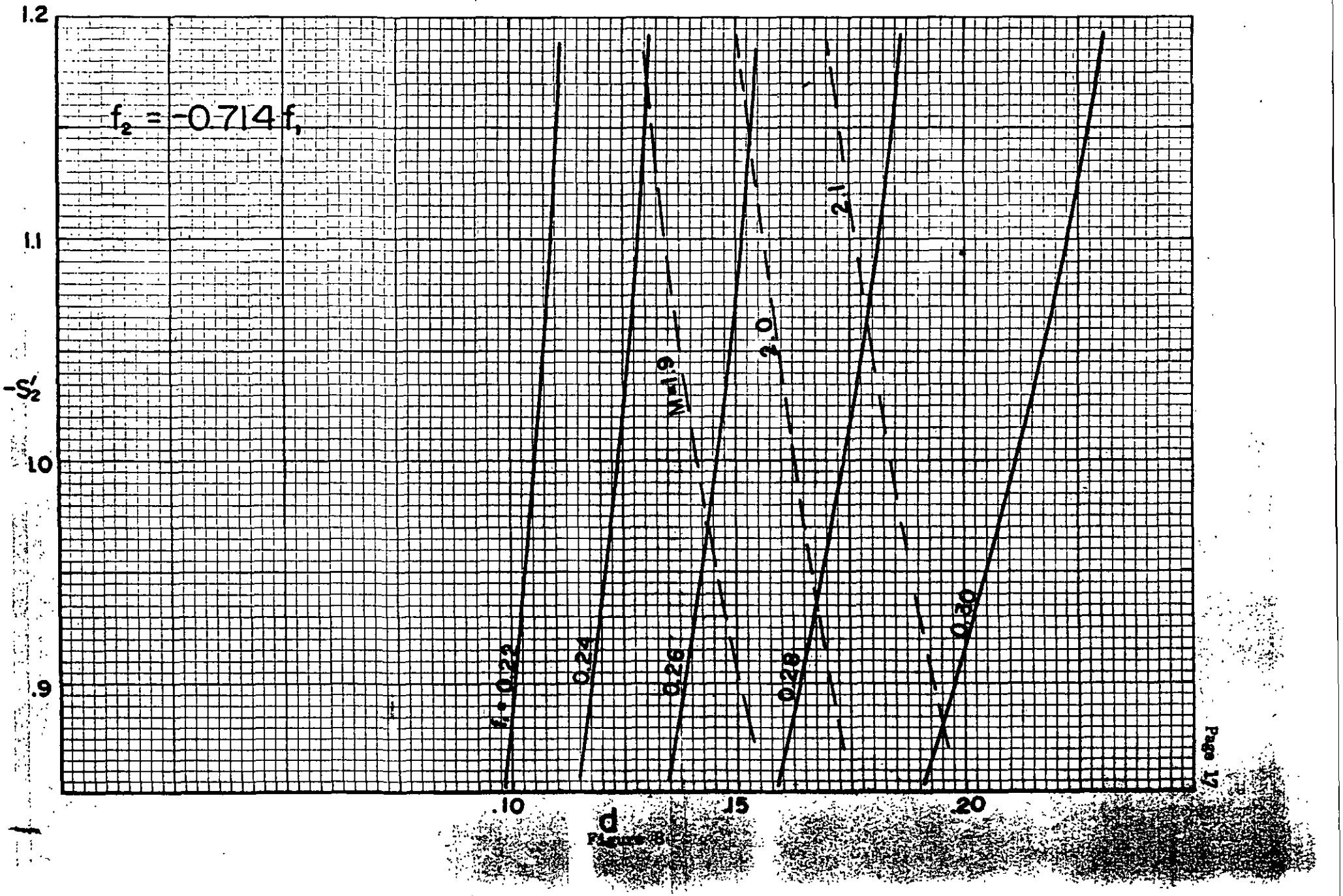

Figure 8

Prints are shown of sample photographs taken with a 23 1/4" lens on an 8" x 10" camera. All photographs include a test pattern of graph paper made with 20 lines to the inch. Kodalith Ortho film was used, and it was not developed to high contrast because, to do so would likely obscure the fine lines. For this reason the images lack the apparent sharpness that one associates with high contrast images. The photographs are made to deliberately show the faults of the optical system. These faults would have been much less apparent if the images showed bold black on white contrast and no very fine lines.

Figure 9 shows the results of adjusting the telescope for a magnification of 1.15 times. There is some lateral chromatism but it is not too apparent unless one scrutinizes the print with a magnifier.

Figure 10 shows the results for a magnification of 1.33. Only blue light was used (Wratten No. 48 filter) but there is still some evidence of lateral chromatism. Also the angular coverage of the telescope is reduced.

Figure 11 is essentially the same as Figure 10 except for the light source. A mercury arc lamp was used with a Wratten No. 47 filter, the combination passing only the 0.405 micron and 0.435 micron lines. This light produced only a spot of light in the middle of the test object. The horizontal lines on the top and bottom of the figure are doubled. The spacing of the lines, as closely as one can measure, agree with the calculated value based on Equation 2 (g) assuming the objective lens is made from common crown glass. The inference to be drawn from Figures 10 and 11 is clear. Excellent results are to be expected at this magnification from a telescope made with simple ophthalmic lenses if monochromatic light is used. If the telescope objective were an achromatic doublet, equally good results should be obtained with any light.

Figure 12 illustrates the result of rotating the telescope about 45° in front of the camera lens. This transforms a square into a parallelogram. The effect this has on the printed letters is called "italicizing" in the graphic arts trade. The maximum italicizing effect occurs when the telescope is rotated exactly 45°, and in this case the angles of the parallelogram differ from the original 90° by an amount:

$$2 \tan^{-1} [(M-1)/(M + 1)]$$

The results shown in Figure 12 are in approximate agreement with the 16 degrees calculated for M = 1.33.

Figures 9 through 12 were all made with a telescope made of lenses 52 mm. in diameter. The focal lengths of the objective and ocular were $\pm$ 67 cm. The limited field of view shown in Figure 10 is simply due to the small diameter of the objective lens. This lens can easily be made of larger diameter to cover a larger field of view.

Figure 13 shows the results with a telescope similar in structure to the one described by the graphs in Figure 8. The magnification is 2.0, which is an extremely high magnification for a telescope made of simple lenses. The illumination was the 0.546 micron green line of a mercury arc. The focal lengths of the objective and ocular were respectively about 37 cm. and -25 cm. An inspection of the image on the ground glass indicated that at this greater magnification, curvature of field becomes important when simple ophthalmic lenses are used. It is believed that the curvature of field problem would be less if the other telescope was used. However, that would have required a greater lens separation D than was possible with the equipment that was used for these tests. It also

would have caused considerable vignetting of the image.

In all of these tests the magnification, as calculated from Equation 2 (c) agreed with the values measured on the original photographic negative.

The test equipment used for these photographs is not described in detail. It was improvised from metal tubing with threaded ends. For professional use the telescope lenses should be mounted on the two ends of a good rigid view camera with bellows, rack and pinion focussing, and a suitable provision for making precise rotational adjustments of the individual lenses. Such an arrangement would enable one to set up the telescope in a very short time.

all/st

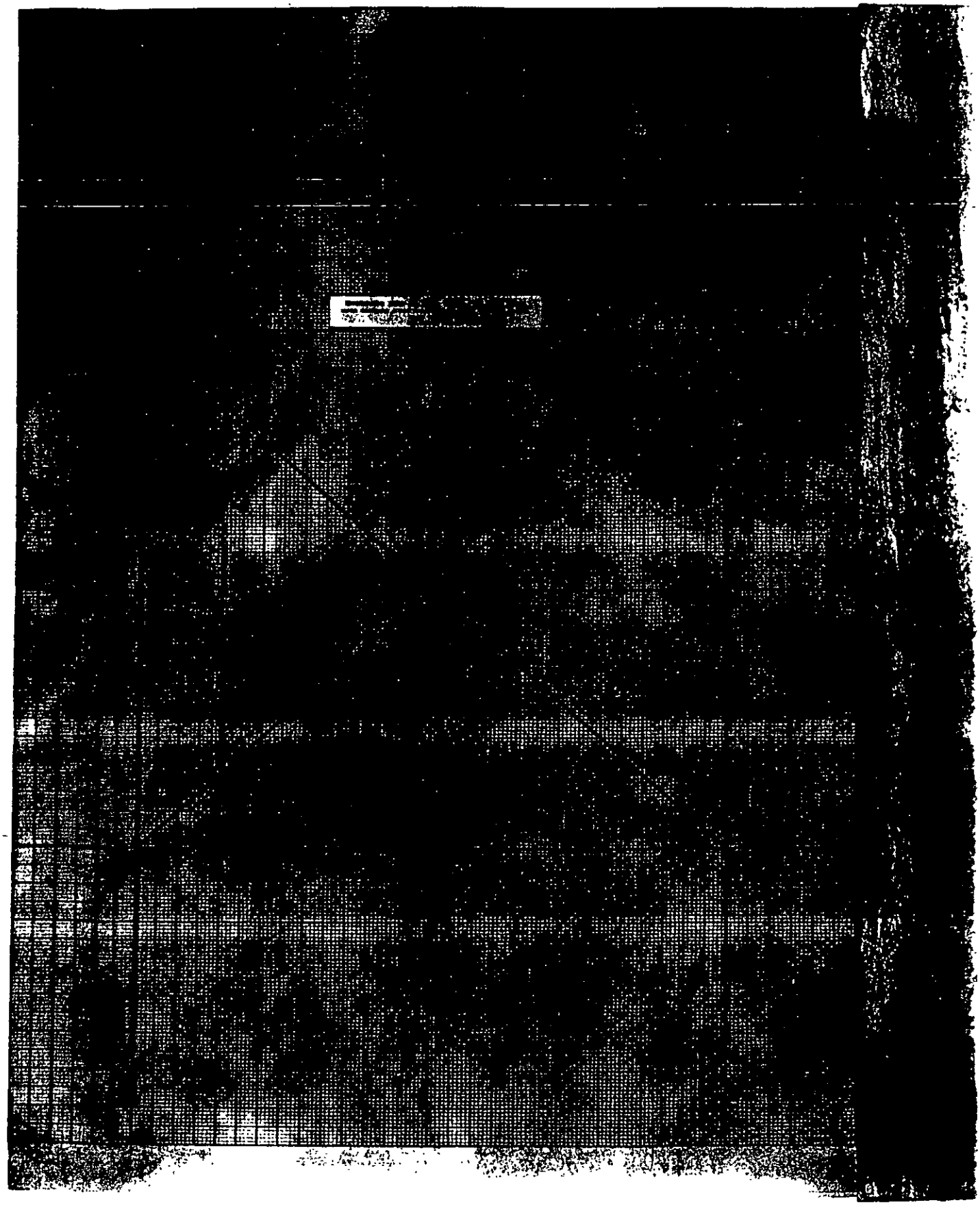

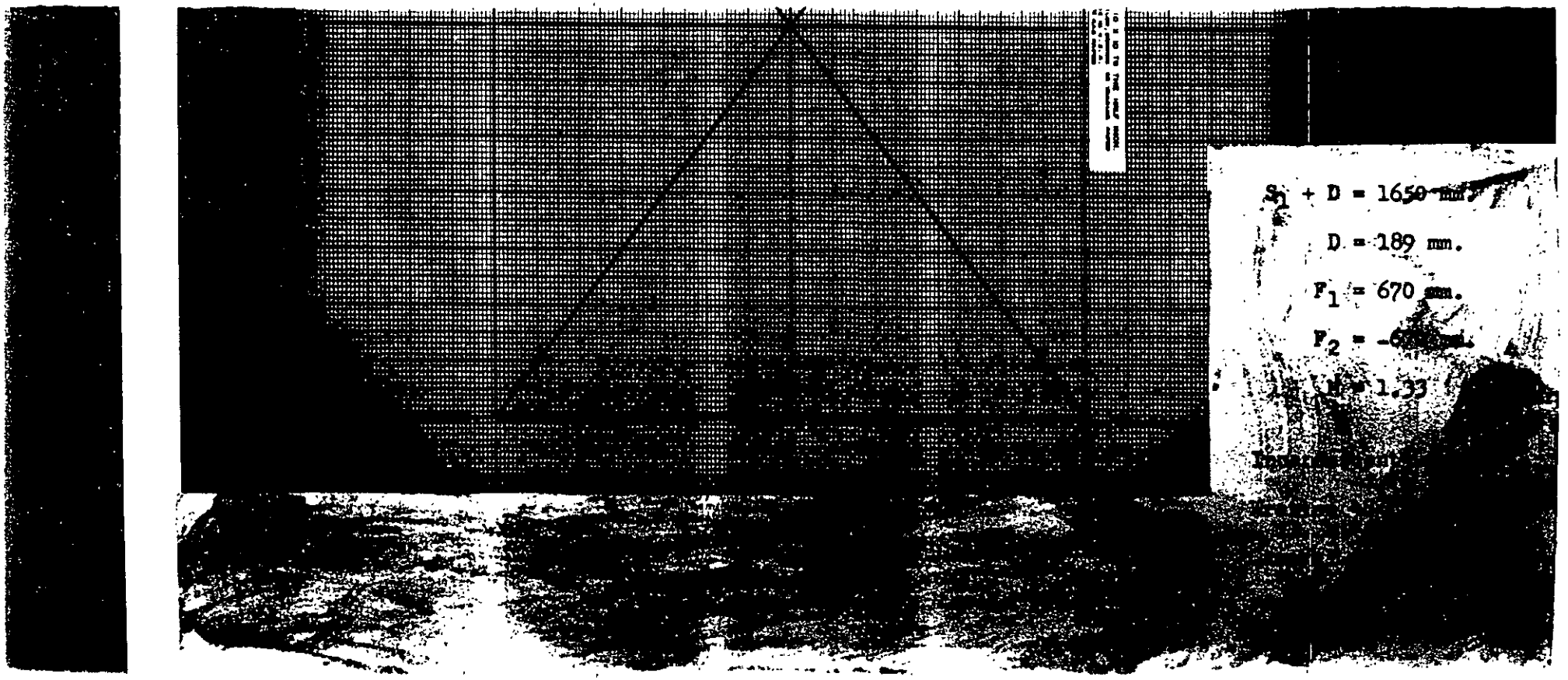
S_1 + D = 1650 mm.
D = 189 mm.
F_1 = 670 mm.
F_2 = -6[illegible] mm.
[illegible] = 1.33

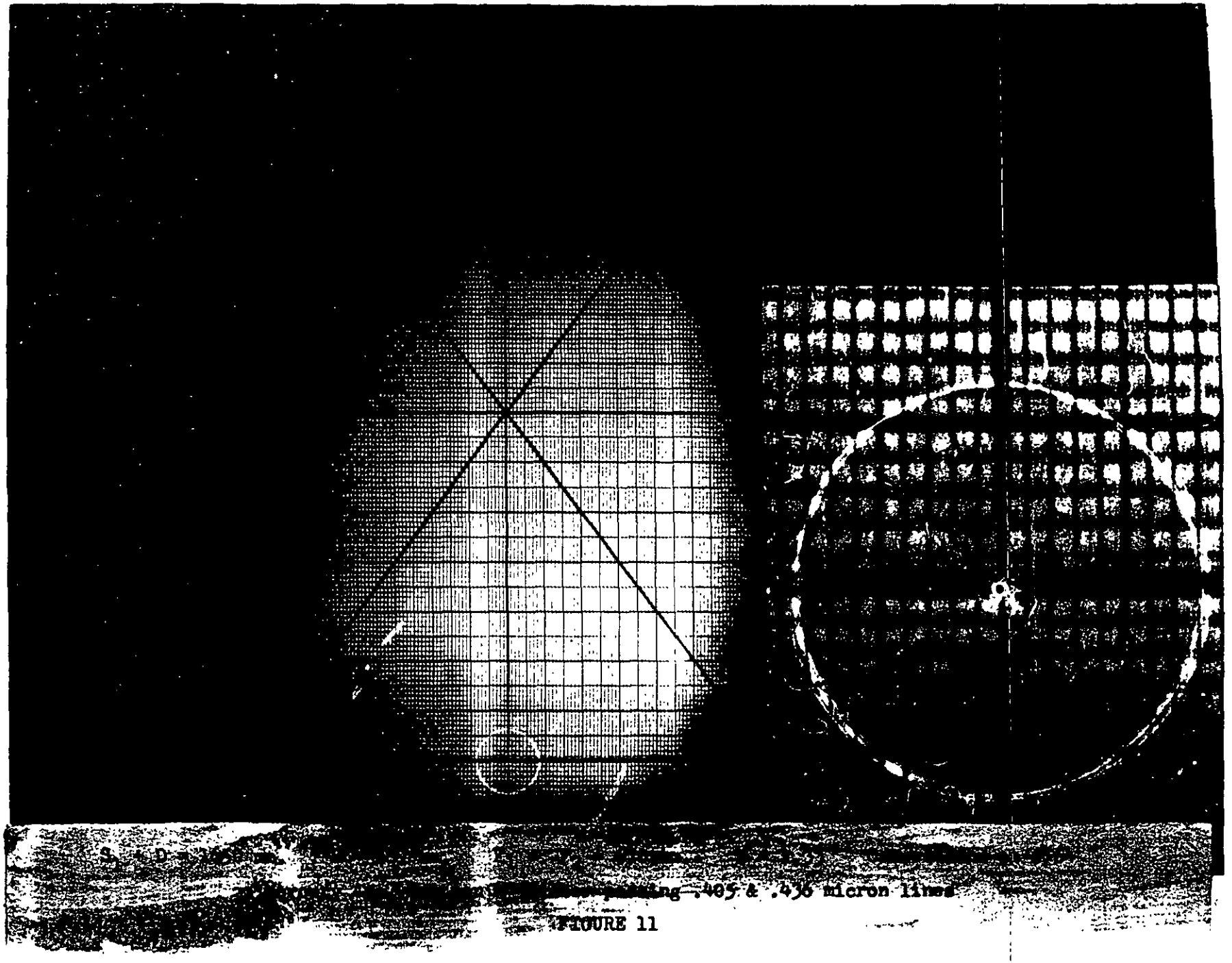

FIGURE 11

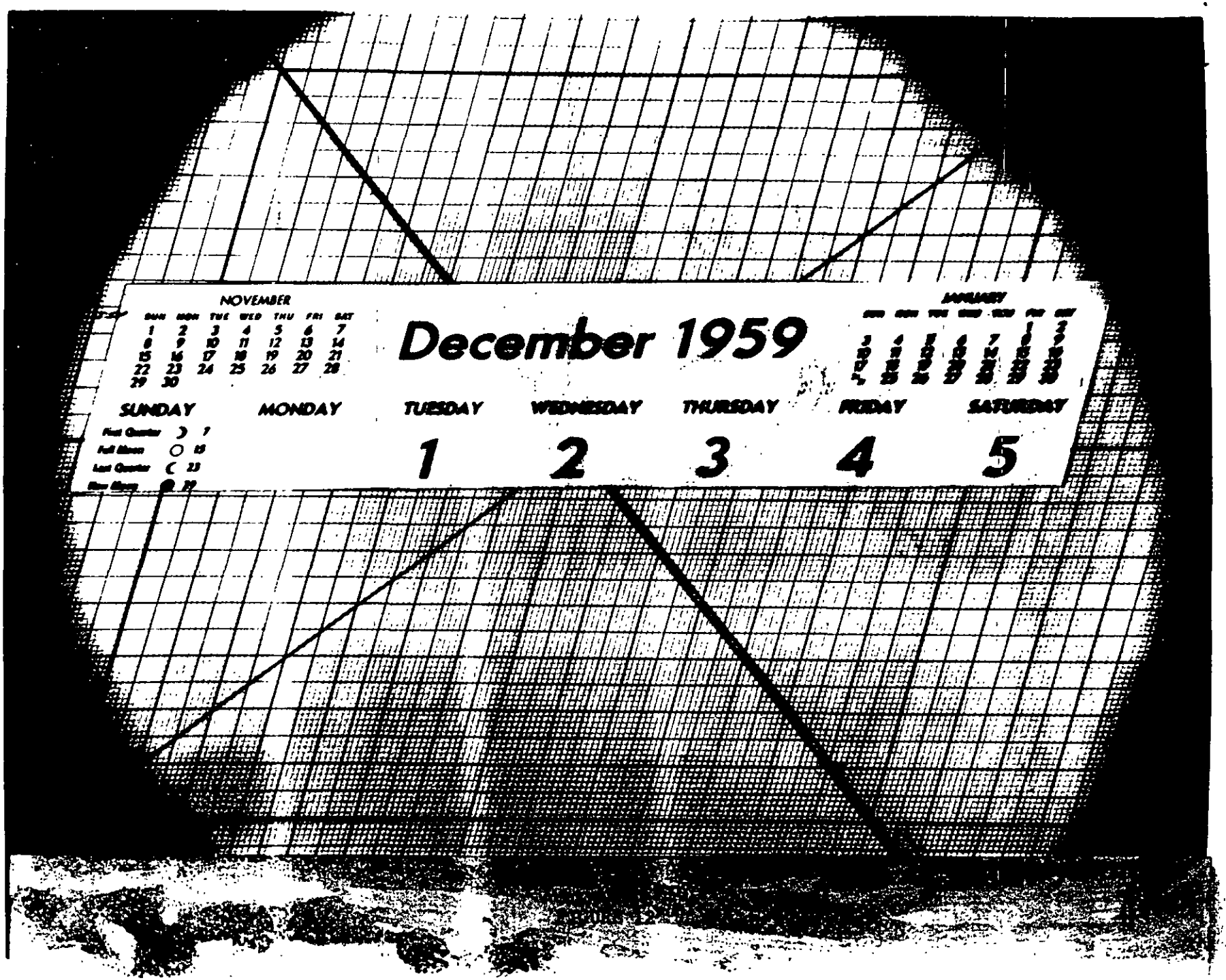
NOVEMBER
December 1959
SUNDAY
MONDAY
TUESDAY
WEDNESDAY
THURSDAY
FRIDAY
SATURDAY
1
2
3
4
5

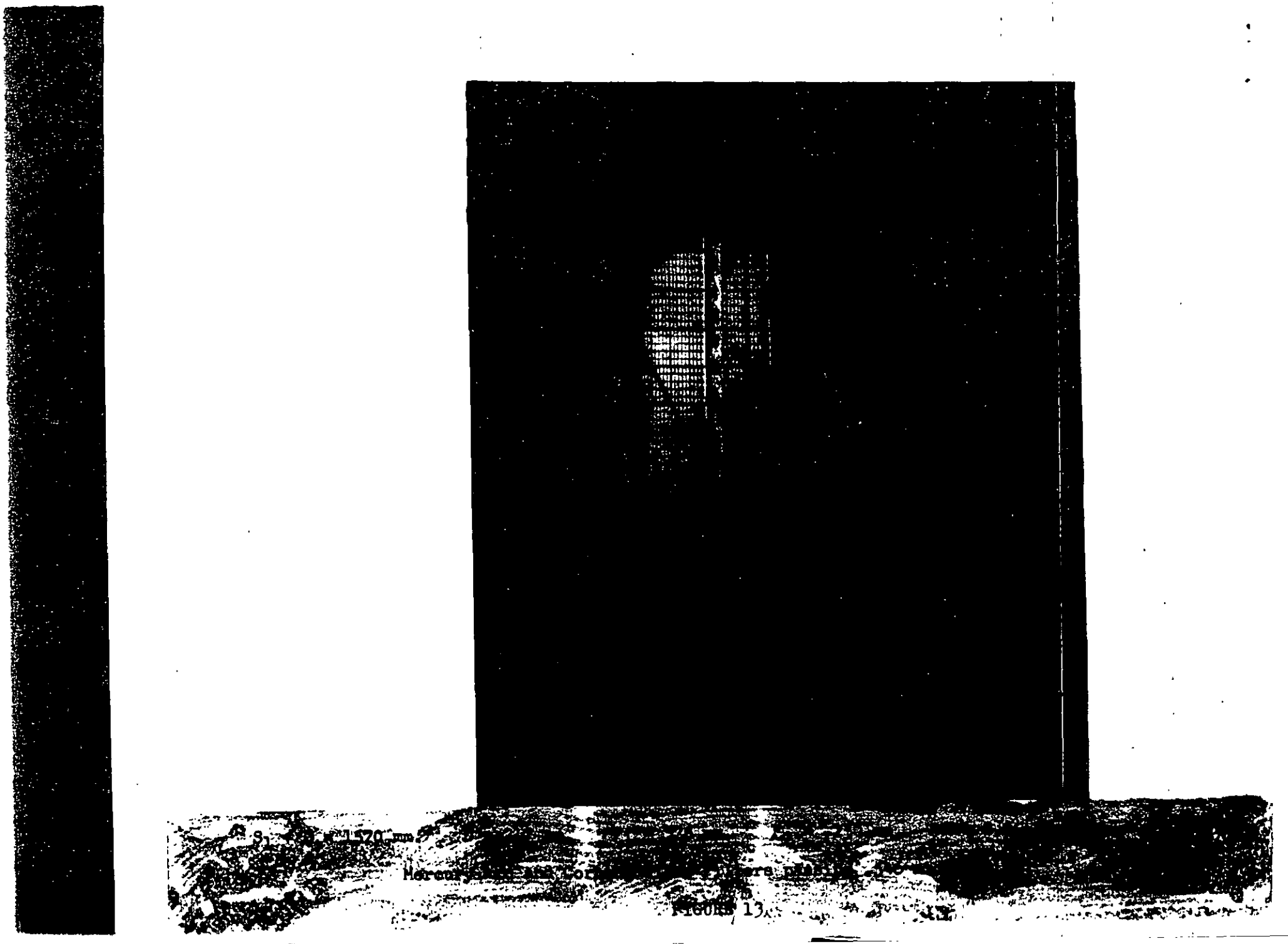

FIGURE 13

PROJECT REPORT FORM

PROJECT NO. 1102-9
COOPERATOR
REPORT NO. 3
DATE September 17, 1963
NOTE BOOK
PAGE TO
SIGNED Arthur L. Lathrop
Arthur Lathrop

Copy to: Files
Reading Copy

PROBLEMS REGARDING THE LIGHT SCATTERING PROCESS

Ed Arnold, as a part of his doctoral research, attempted to compute theoretically the Kubelka Munk scattering coefficient of a glass fiber mat. The attempt was conspicuously unsuccessful. His computed coefficient was about 2 or 3 times too great, depending on the detailed assumptions made in making a connection between the individual glass cylinders and the hypothetical "infinitesimal" layer. Further work was done by Lathrop on this problem and has been submitted as a Project 2210 report. This work shows that the discrepancy in Arnold's work will remain as long as his general method of attack is used. That is, it does not appear possible to clear up the difficulty by juggling the assumed angular distribution of the diffuse radiation inside the sheet.

Consequently, it seemed advisable to consider a totally different method of attack. As a working hypothesis the Kubelka Munk model, itself, has now been rejected. A varied model has been given by Duntley (Jour. Opt. Soc. Am. pg. 61, vol. 32, Feb. 1942). The first indications are that this model may resolve the difficulties that Arnold observed, and further may give a valuable method for further study of the mechanism of light scattering and absorption in layers of powdered or fibrous materials. Some measurements have been made on tea bag paper and translucent drafting paper. In both cases fairly small but definite departures from the predictions of Kubelka Munk are observed. Further, these departures are in exactly the direction that Duntley's theory would indicate. Also, a

consideration of Duntley's theory suggests that the Kubelka Munk results will be most nearly correct for small particle scattering centers that approach Rayleigh law scatterers. Conversely, large particle scatterers have a marked preference for scattering in the forward direction; and these materials should show the greatest departures from the predictions of the Kubelka Munk Theory.

The Duntley model is based on a consideration of what happens in a reflection meter like the General Electric Recording Spectrophotometer, in which the incident light beam is collimated and the diffuse reflected light is collected in an integrating cavity. Duntley assumes that the total radiation incident on any infinitesimal layer can be divided into two parts, a collimated part and a diffuse part. Consequently, there are two scattering coefficients B & B' analagous to the K.M. scattering coefficient, s. Similarly, there are two absorption coefficients μ and μ' analagous to the K.M. k coefficient. In each case the primed quantity refers to an incident collimated beam. Further, a coefficient, F', describes the part of the forward travelling incident collimated flux that is converted to forward traveling diffuse flux. In the Duntley model all of the back scattered flux is diffuse flux. Calculations made by Lathrop and Arnold, as well as others, would suggest that $B > B'$ and $\mu > \mu'$. Also, it is likely that $F' > B$. The usual viewpoint taken with respect to the Kubelka Munk theory is simply that the incident light becomes diffuse light almost immediately upon penetrating the light scattering medium. If this were true, then $F' >> B > B'$. A cursory check shows immediately that the Duntley equations reduce to the K.M. equations in that special case. [Of course, the Duntley equations also reduce to the K.M. equations when $B = B'$ and $\mu = \mu'$.]

The difference between a "Duntley scatterer" and a K.M. scatterer is readily shown in two graphs. Let us plot the reflectance and transmittance against sheet weight. The results are generally

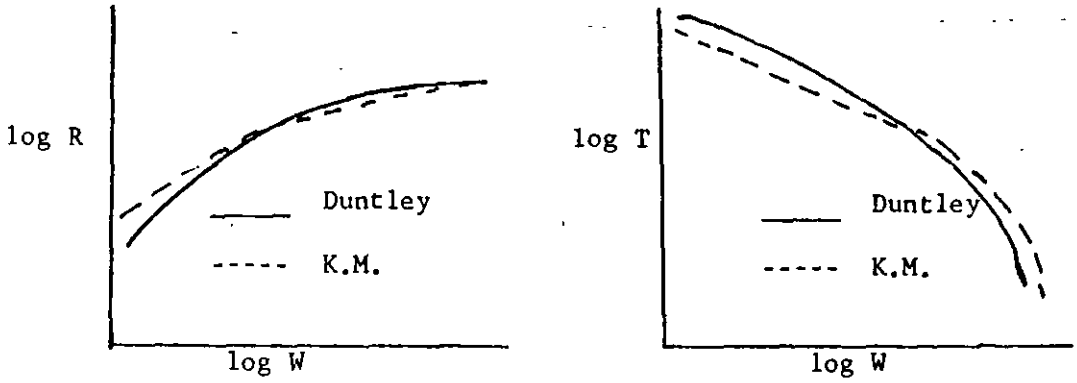

of the nature shown--assuming $B > B'$ and $\mu > \mu'$. Measurements made on two different papers, as mentioned before, confirm that the Duntley theory gives a much better description of the observed results. For example, in the case of the tea bag paper, the observed results are very closely described by the coefficients s = 0.4 k = 0.021. However, this description holds best only for the heavier weights. For one or two individual sheets where Ro is in the range of 0.25 to 0.40, the Kubelka Munk predictions are off by about 2 points in both Ro and T. Of course, if both s and k are raised proportionally one gets a better fit for the light weights and a poorer fit for the heavier weights. The same material in Duntley terms is described by B = 0.44, B' = 0.36, μ = 0.0197, μ' = 0.013, and F' = 0.68. For the tracing paper the results are similar but the ratio of B to B' is somewhat greater than in the case of the tea bag paper. If there are any systematic errors in the Duntley description, the photometric accuracy of these tests (random irregularities of about 0.3 points) is insufficient to show it.

Planned for the future are tests with pulverized or fibrous glass mats. It is expected that with glass fibers as large as Arnold's,

the ratio of B to B' should be much greater, perhaps as great--or greater than 3 or 4 to 1. What is known of the angular scattering distribution of cylinders and spheres suggests this. As a hypothetical problem consider a glass fiber mat with $R_\infty = 0.8$. As one possible case the Duntley coefficients could be B = 2.7, B' = 0.657, $\mu = 0.0162$, $\mu' = 0.0108$, and F' = 1.186. A scattering sheet that followed this description could also be described--for the heavier weights--by the Kubelka Munk coefficients s = 1.0 and k = 0.025. The case proposed is purely "out of the hat," but if such a material did exist it would explain Arnold's results. What Arnold calculated is more closely related to the Duntley coefficient B than it is to the Kubelka Munk coefficient, s. Further, in the case suggested, the values of Ro, T_s and R_∞ are very closely in accord with the Kubelka Munk predictions when Ro is near 0.70. Only by checking a vareity of weights, particularly the lighter weights, would it be apparent that the Kubelka Munk theory was seriously wrong.

There is one point of interest in the measurements that have been made on the papers tested and in the hypothetical problem mentioned above. In almost all cases one gets the best fit by taking a Kubelka Munk absorption coefficient greater than either μ or μ'. Also in some of the hypothetical problems it is observed that the sheet reflectance decreases when the coefficient B increases--that is, dR/dB is negative. Both of these observations may be manifestations of a light "trapping" effect. This would occur only when the ratio B/B' is substantially greater than unity. In that case the incident collimated beam would find it easy to enter the sheet because B' is relatively small. The back scattered light would find it harder to get back out of the sheet because B is relatively large. This observation, in the absence of a more formal scrutiny

of the mathematical relationships, would serve as an explanation for the negative value of dR/dB and also for the fact that the best fit to the Kubelka-Munk theory demands a high value of the absorption coefficient k.

This peculiarity of the absorption coefficient k, also suggests a possible result for an experiment that has been considered before. That is the experimental check of the relationship between the Kubelka Munk coefficient k, and Bouguer's law absorption coefficient α. Van den Akker calculated that k/α would equal 2, at least if certain conditions implied in the calculation were met. It is likely that with large particle scattering the "trapping" effect is greater and the Kubelka Munk coefficient is substantially greater than Duntley coefficients μ or μ'. Similarly, then, one might expect that the Bouguer law absorption coefficient is more closely related to μ and μ' than it is to the Kubelka Munk coefficient, k. Then the ratio k/α would be greater for large particle scattering mats than for small particle mats.

It's risky, of course, to really try to predict in advance the result of experimental tests. In preparation for the planned experiments an inquiry has been made of Corning Glass Works about fibrous and pulverized colored glass. So far no reply has been received. Also an integrating cavity is being prepared, for use with our photo multiplier photometer. This would enable one to check these two scattering theories at low values of transmittance that are outside the range of the G. E. R. S. Also a different instrument would make it feasible to use pulverized glass mats. It is not practical to use these on the G. E. R. S. because the mat must be held in a vertical plane and would be apt to fall into the integrating cavity.

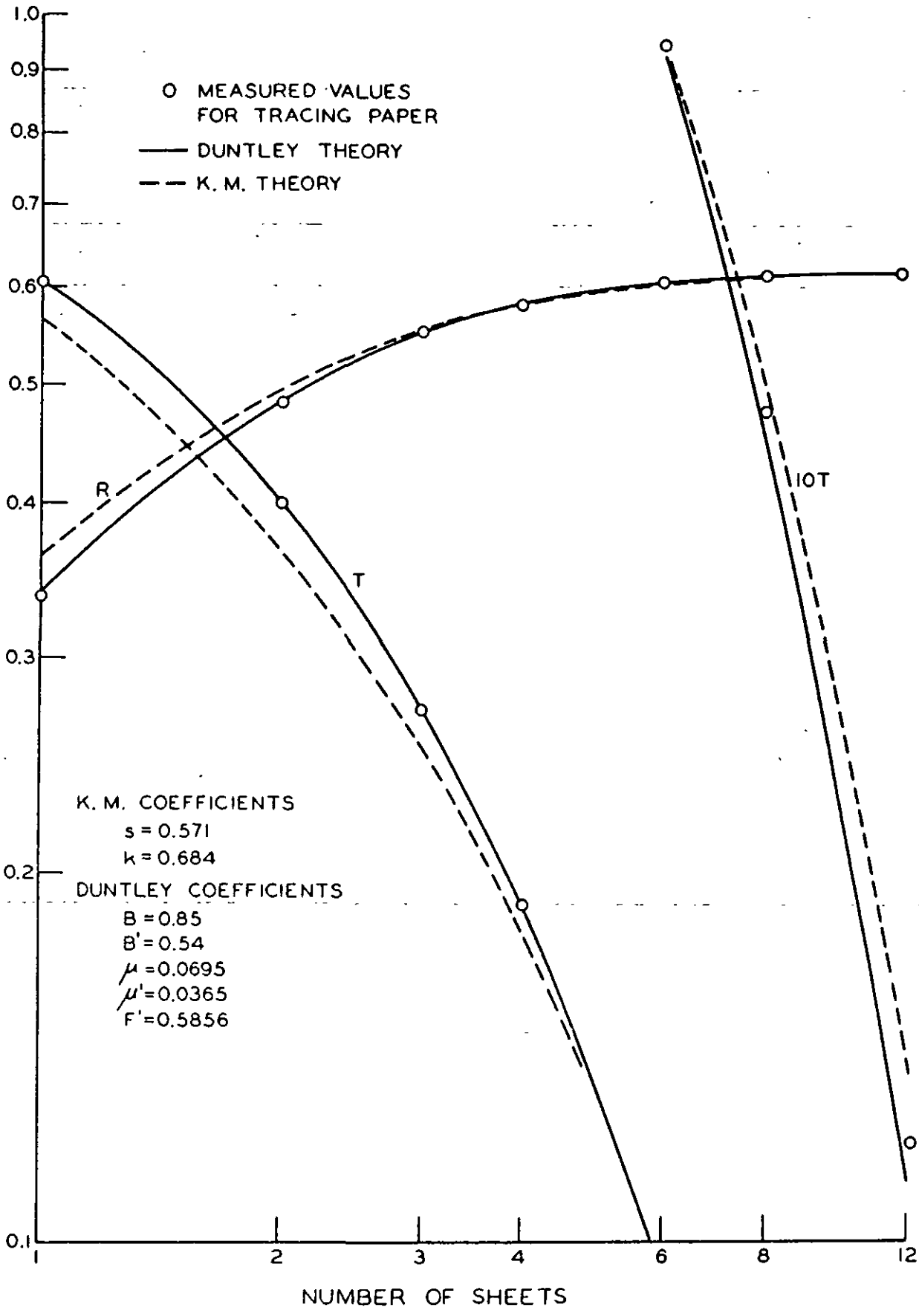
1.0
0.9
0.8
0.7
0.6
0.5
0.4
0.3
0.2
0.1
O MEASURED VALUES FOR TRACING PAPER
DUNTLEY THEORY
K. M. THEORY
R
T
10T
K. M. COEFFICIENTS
s = 0.571
k = 0.684
DUNTLEY COEFFICIENTS
B = 0.85
B' = 0.54
μ = 0.0695
μ' = 0.0365
F' = 0.5856
1
2
3
4
6
8
12
NUMBER OF SHEETS

PROJECT REPORT FORM

PROJECT NO. 1102-9
COOPERATOR Institute of Paper Chemistr
REPORT NO. 4
DATE August 25, 1967
NOTE BOOK
PAGE TO
SIGNED Carl E. Scheie
Carl E. Scheie

Copies to: Files
D. Johnson
Sell
Scheie
Weiner

NUCLEAR MAGNETIC RESONANCE STUDIES OF PLASTIC SOLIDS

INTRODUCTION

A full investigation of any solid will embrace measurements of both the NMR spectrum and the spin-lattice relaxation time. The information obtained from the two measurements is as follows:[1]

1. It is possible to tell whether a molecule or group is rotating.
2. The nature of the rotational motion can be determined.
3. The temperature dependence of the rate of motion can be determined.
4. The diffusion of molecules in the solid and the temperature dependence of the migration rate can be determined.

The purpose of the present investigation is twofold. First, to acquaint the investigator with NMR techniques and secondly, to check the feasibility of using the Varian A-60A NMR Spectrometer at The Institute of Paper Chemistry to make the above mentioned measurements.

PLASTIC SOLIDS

Certain molecules form plastic crystals when freezing from the liquid state. These molecules are called globular molecules because they are approximately spherically symmetric (methane) or appear to be spherically symmetric because of rotation (cyclohexane).[2] Plastic crystals have a crystal structure with a high degree of symmetry, usually cubic. This is often called the high temperature or rotor phase. At a lower temperature, these solids undergo a solid-solid transformation to a less symmetrical crystal form and assume physical properties more generally associated with solids. The entropy of fusion of the plastic solids is less than 5 e.u. The sum of the entropies of fusion and transformation of plastic solids is about the same as the entropy of fusion for a similar but nonplastic solid. For example, the entropy of fusion for benzene is 8.5 e.u. The entropy of fusion for cylcohexane is 2.2 e.u. but the entropy of transformation is 8.6 e.u. Because of the unique properties of these solids one anticipates that they would offer an opportunity to study a substance which lies somewhere between the liquid and the solid state.

The rotational behavior of polar molecules in the solid state has been verified by dielectric measurements[3] and more recently that of nonpolar molecules by NMR measurements.[4] Elastic moduli, calculated from velocity of sound measurements, seem to support the assumption that the molecules can be treated as being spherically symmetric due to their rotational motion.[5]

Plastic crystals should not be confused with liquid crystals. In normal solids, when the temperature is high enough, the thermal energy is of such a

magnitude that the crystal boundaries are broken and the substance liquifies. Simultaneously, the free molecules assume random orientations giving an isotropic liquid. In plastic crystals the freedom to rotate (isotropy) already exists in the solid state but the coherence of the crystal is broken only at the melting point. In liquid crystals, the fluidity comes first, giving an anisotropic liquid.

In addition to their pseudo-solid nature which is interesting in itself, the rotational motion of the molecule affords an excellent opportunity to develop techniques and analysis which can be applied to other systems. For example, the temperature dependent properties of crystalline polymers are often dependent on the behavior of groups along the chain.[6] The motion of these groups is similar to the hindered motion of the globular molecules. Although a great deal of effort is being expended in this area, the success has not been overwhelming because of the complexity of the system.

NMR IN SOLIDS[7,8,9]

Pauli suggested that the splitting of spectral lines might be explained by assuming nuclei possess spin angular momentum and a magnetic moment. We know that the maximum possible value of the component of the nuclear angular momentum in any direction is $\hbar I$, where I is the spin quantum number. All data on nuclei are consistent with the idea that the magnetic moment is zero if $I = 0$, and if $I \neq 0$, the moment is parallel to the angular momentum vector;

$$\vec{\mu} = \gamma \hbar \vec{I} \qquad (1)$$

where γ is a constant.

We know the following about nuclei:

1. If the mass number A is odd, I is half integral.
2. If the mass number A and the charge number Z are both even, I = 0.
3. If A is even and Z is odd, I is an integral.

We see that carbon 12 has I = 0 but the hydrogen nucleus has $I \neq 0$. If I = 0, there is no NMR spectra.

If the nucleus that possesses a magnetic moment is introduced into a magnetic field H_o, the energy of interaction is given by

$$U = -\vec{\mu} \cdot \vec{H}_0. \qquad (2)$$

Choosing the z axis along $\vec{H}_o$

$$U = -\mu_z H_o = -\gamma \hbar H_o I_z. \qquad (3)$$

I can take on the values I, I-1, ..., - I+1, -I. Since protons have spin 1/2,

$$U = \pm \gamma \hbar H_o/2. \qquad (4)$$

Thus the two energy states are separated by $\gamma \hbar H_o$. If a radiative transition occurs between these levels,

$$\hbar\omega_o = \gamma \hbar H_o,$$

and

$$\omega_o = \gamma H_o. \qquad (5)$$

For a proton, $\gamma = 2.68 \times 10^4$ sec^{-1} gauss^{-1}

and $\mu = 1.410 \times 10^{-23}$ erg/gauss.

The basis of NMR experiments is to induce transitions between these two levels by absorption or emission of energy. The frequency of this energy is, $f = \gamma H_o/2\pi$. For a proton in a field of $H_0 = 10^4$ gauss, f = 42.6 MHz. This is in the radio frequency range.

Thus far we have ignored any environmental effects, i.e., we have assumed all the nuclei experience the same magnetic field H_o. This is not the case in real life because of the effects of the neighboring nuclei. However, if the surrounding nuclei are in rapid motion, as in a gas or liquid, the effects of neighbors averages out to be just about zero, giving absorption lines that are very sharp. There is not an averaging process in the case of solids and the lines are much broader. The line width is used to obtain information about the molecular motion and molecular geometry.

When our collection of nuclei is in thermal equilibrium at some temperature, T, the lower energy state will be more populated. If N_1 is the population in the lower level and N_2 the population in the upper level, the ratio N_2/N_1 is given by the Boltzmann factor.

$$N_2/N_1 = \exp(-2\mu H_0/kT), \qquad (6)$$

where k is the Boltzmann constant. At room temperatures and $H_o = 10^4$ gauss, $2\mu H_o/kT \sim 10^{-5}$.

The spinning proton (nucleus) in a magnetic field experiences a torque equal to the rate of change of the angular momentum of the system.

$$d(\vec{\hbar I})/dt = \vec{\mu} \times \vec{H} \qquad (7)$$

$$d\vec{\mu}/dt = \gamma \vec{\mu} \times \vec{H} \qquad (8)$$

This is for one nucleus. If there are more than one we sum over them all per unit volume. This yields the nuclear magnetiziation, M.

$$\vec{dM}/dt = \gamma \vec{M} \times \vec{H}. \qquad (9)$$

If H is again directed along the z axis,

$$M_z = M_o = \chi_o H_o \qquad (10)$$

where χ_o is the magnetic suspeptibility. The magnetization is related to the population difference $N_1 - N_2$.

$$M_z = \mu(N_1 - N_2) \qquad (11)$$

for systems with spin 1/2.

If we are not at thermal equilibrium,

$$dM_z/dt = (M_o - M_z)/T_1, \qquad (12)$$

i.e., we assume M_z approaches equilibrium at a rate proportional to the departure from the equilibrium value of $M_o = \gamma H_o$. T_1 is called the spin-lattice relaxation time. It is a measure of the rate at which the spin system comes into thermal equilibrium with the other degrees of freedom.

Suppose we rotate the vector $\vec{\mu}$ with an angular velocity whose magnitude and direction are given by $\vec{\omega}$.

$$d\vec{\mu}/dt = \vec{\omega} \times \vec{\mu} \qquad (13)$$

Comparing equations 8 and 13 we see that the effect of the magnetic field is exactly equivalent to a rotation with angular velocity

$$\vec{\omega} = -\gamma \vec{H} \qquad (14)$$

Thus if H_o is constant, the magnetic dipole will precess about the direction of H_o with an angular frequency $-\gamma H_o$. This is commonly referred to as the Larmor frequency.

If a second magnetic field H_1 of constant magnitude and direction perpendicular to H_o is introduced, a torque $\vec{\mu} \times \vec{H}_1$ will be exerted on the nucleus. As the frequency of the H_1 field approaches that of the precession

frequency the resultant torque approaches a constant value and this will show up as a resonance phenomenon. The energy absorbed from the H_1 field, at resonance, is exactly the frequency required to induce transitions between the two spin states.

As was stated earlier the absorption does not occur at a single frequency but over a range of frequencies. This broadening of the spectral line is due to a variety of causes the most important being spin-lattice relaxation and magnetic dipole broadening. The former is most important in liquids and gases and the latter in solids. Spin-lattice relaxation results from the interaction of neighboring magnetic dipoles as the nuclei move relative to one another. In this way the energy is transferred to the spin system from the translational and rotational degrees of freedom. The order of magnitude of the broadening can be estimated from the uncertainty principle.

$$\Delta E \, \Delta t = \hbar. \qquad (15)$$

Since, $\Delta E = U = \hbar \Delta \omega$

This implies, $\Delta f = 1/(2\pi \Delta t)$. Thus the line width on a frequency scale will be of the order of $1/T_1$.

If the nuclei remain in the same relative positions for a long time, as in solids or viscous liquids, we have to treat them as being in a variety of local magentic fields. The line width in this case is characterized by a time T_2, smaller than T_1. T_2 and T_1 become equal when the molecules are

rotating rapidly so the magnetic field averages out.

In practice, the line width is defined as the width between the maximum and minimum of the derivative of the absorption line. It turns however, that the second moment of the line about the zero of the first derivative is a more useful quantity.

PRESENT INVESTIGATION

The NMR spectrometer available at The Institute of Paper Chemistry is a Varian A-60A. This instrument was designed for use with liquid samples, primarily in solution. However, because of the high degree of motional freedom of the molecules in plastic solids it was anticipated that this apparatus could be used to study this motion. One of the objectives of this investigation was to see to what extent this would be possible. The A-60A is classified as a high resolution instrument in contrast to a wide line instrument. Almost all of the previous work on solids has been done on wide line instruments but there has been a desire to extend the investigation into the high resolution region.

The particular solids chosen for this study were cyclohexane, camphene, and cyclohexanol. A summary of some properties of these solids is shown in Table I.

Table I. Physical Data for Solids Investigated.

	Cyclohexane	Camphene	Cyclohexanol
Temperature of Fusion (°C)	6	50	25

Table I. Physical Data for Solids Investigated (Continued)

	Cyclohexane	Camphene	Cyclohexanol
Entropy of Fusion (e.u.)	2.4[10]	2.3[11]	1.4[12]
Crystal Structure	fcc	bcc	fcc
Transformation Temperature (°C)	-86	-120	-8 -28
Entropy of Transformation (e.u.)	8.6[10]		7.4[12]

The basis for selecting these particular solids was not arbitrary. On the other hand, they are not thought to be unique in their characteristics so the conclusions drawn from the work should possess some generality. Cyclohexane has been studied using wide line instruments.[13] This should provide a check on the results. The spectrum of cyclohexane shows a single line which makes the data reduction a relatively simple task. The high resolution investigation may also produce some fine structure which would not show up in the wide line experiments. The 90°C interval between the melting and transformation temperatures is very desirable when studying thermal variations.

Camphene is of interest as a comparison with cyclohexane since it has a bcc structure in the plastic state as opposed to the fcc structure for cyclohexanol. The plastic state exists from +50° to -120°C allowing meaningful thermal variations to be studied. It is known that fcc structures are more stable than bcc structures[14] and one would expect this to be evident from the

NMR data. Although neither melting nor phase transitions have been predicted from stability conditions, if the exact nature of the motion of the molecules was known it would surely shed some light on the subject.

Elastic constant measurements indicate that the solid-solid transition for cyclohexane is abrupt (this is also true for cyclohexanol which is also fcc). In the case of camphene there appears to be an "easing into the transition."[5] However, these measurements do not reflect the whole picture since they are concerned only with the vibrational motion of the molecules. The Debye temperature determined from ultrasonic techniques is almost a factor of three larger than that determined from x-ray techniques,[15] which are sensitive to both vibrational and rotational motion. The Debye temperature is not a good way to express the results of motion in the solid but it does give an indication as to the types of motion. The NMR data for cyclohexane show that in addition to the vibrational and rotational motion there is a translational motion of the molecule as well. This is called self-diffusion and occurs down to about -40°C. From x-ray and density data on camphene one would predict self-diffusion sets in at about -20°C. This should be easily detected from the line width measurements on the NMR spectra. There has not been any reference to NMR investigations of camphene in the literature.

Cyclohexanol is an interesting solid in that it exists in three solid states. The phase transformations have been thoroughly studied and described as follows:[16]

Phase I, the plastic crystalline phase, is stable from the melting point (25°C) down to -8°C. However, if it is cooled fast enough, phase I can be supercooled down to liquid nitrogen temperatures. If it is cooled more slowly it will undergo a transition to phase II between -55°C and -70°C. Phase II is metastable and transforms back to phase I at -28°C. Phase III is the stable low temperature modification and can be obtained from either phase I or II provided there are some phase III nuclei present. Phase III transforms back to I at -8°C.

There is no difference between phases II and III as determined from dielectric constant measurements other than the temperature at which the transformation to phase I occurs. If the intra- and intermolecular motion of the molecules can be determined from the NMR measurements as a function of temperature the difference between the transitions to these two low temperature states should be apparent.

There are two references to previous work on the NMR spectra of cyclohexanol. The first[17] using wide line apparatus is confusing because more than one phase was present while the measurements were made. Furthermore, it appears that it was not known exactly which phases were present. A later study,[18] using high resolution apparatus, reports only the temperature variation of the spectra in phase I down to -9°C. Their only conclusion was that self diffusion must occur in phase I.

The spectra of both camphene and cyclohexanol show three well resolved peaks in the plastic state just below the melting point. This is very advantageous in determining the exact nature of the motion of the molecule, i.e., as the temperature is lowered the rotational motion of the molecule will probably be more hindered and tend to be directed more and more in a given direction.

RESULTS AND DISCUSSION

The present results seem to indicate that the A-60A spectrometer is not ideally suited for investigations of plastic solids. The exact cause of the difficulties is not understood; however, in the course of the investigation experimental techniques were improved allowing measurements to be made which were not possible in the initial stages of the program. The most frustrating and, as yet, unexplainable finding was that the signal for both cyclohexane and cyclohexanol disappears as the temperature decreases. In both cases the disappearance occurs at temperatures well above the solid-solid transformation temperature. One possible explanation could be the following. The samples are cooled by a stream of dry nitrogen gas which is cooled by circulating through a liquid nitrogen bath and later heated by an electric heater in the NMR probe. If the heating is not constant, i.e., the heater goes on and off, there exists the possibility of having cold blasts of nitrogen imposed on the sample tube. This cold blast could cause the sample to be cooled to a point where it would begin to transform to the lower solid state. The needle on the temperature controller does oscillate to some degree indicating that the temperature is fluctuating somewhat. The people at Varian do not feel that such blasts do occur. When the heat exchanger between the nitrogen gas and the liquid

nitrogen was replaced by a less efficient model, it was possible to go lower in temperature before the signal disappeared. This is consistent with the cold blast theory. Furthermore, the needle fluctuation was not as pronounced with the less efficient exchanger.

Changes in temperature also effect the geometry of the instrument and in turn the magnetic field. To compensate for this, a methanol standard was inserted into the probe at each temperature and the instrument was tuned. In doing so, the sample under investigation has an opportunity to collect moisture on its tube. This condensate must be avoided and every effort was made to do so.

The line width of cyclohexane at -30°C, as determined in the present investigation, is the same as that reported in the literature, 0.47 gauss. This is the only check point we have at this time since -30°C is the lowest temperature at which a signal has been recorded for cyclohexane in this study and the highest temperature at which a reliable value can be determined from the literature. It should be pointed out that the values at -10°C agree as best as can be determined.

Figure 1 shows a portion of the absorption curve for cyclohexane at about -20°C. The narrow peak is characteristic of a liquid. The broad line is characteristic of a solid (a normal solid, nonplastic, would have a much broader line than this). The origin of the superposition of the two lines is not known. There is no mention of the occurrence of this phenomenum for

cyclohexane in the literature. This is undoubtedly due to the fact that the wide line spectrometers would not respond to such a narrow peak. The superposition occurred down to the temperature where the signal disappeared and the relative amplitude of the narrow and broad portions of the curve remained about equal.

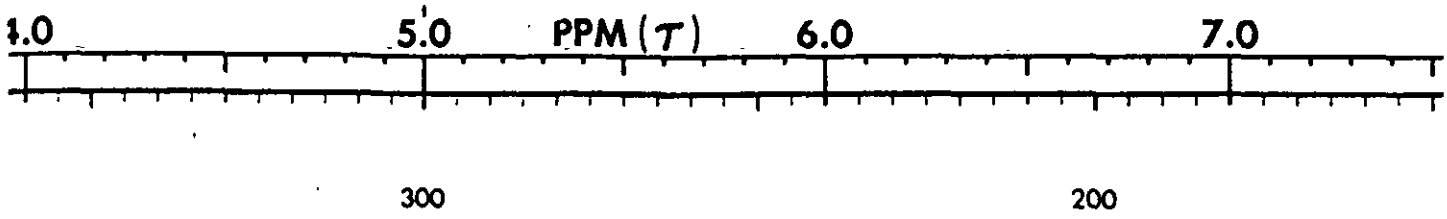

300 200

SOLVENT	– – –	– – –		
TEMPERATURE	Q-26	– – –	°C	
FILTER BANDWIDTH	4	– – –	cps	
R.F. FIELD	0.04	– – –	mG	
SWEEP TIME	250	– – –	sec	
SWEEP WIDTH	1000	-500 – –	cps	
SWEEP OFFSET	-100	– – –	cps	
SPECTRUM AMP.	32	– – –		
INTEGRAL AMP.	– – –	– – –		

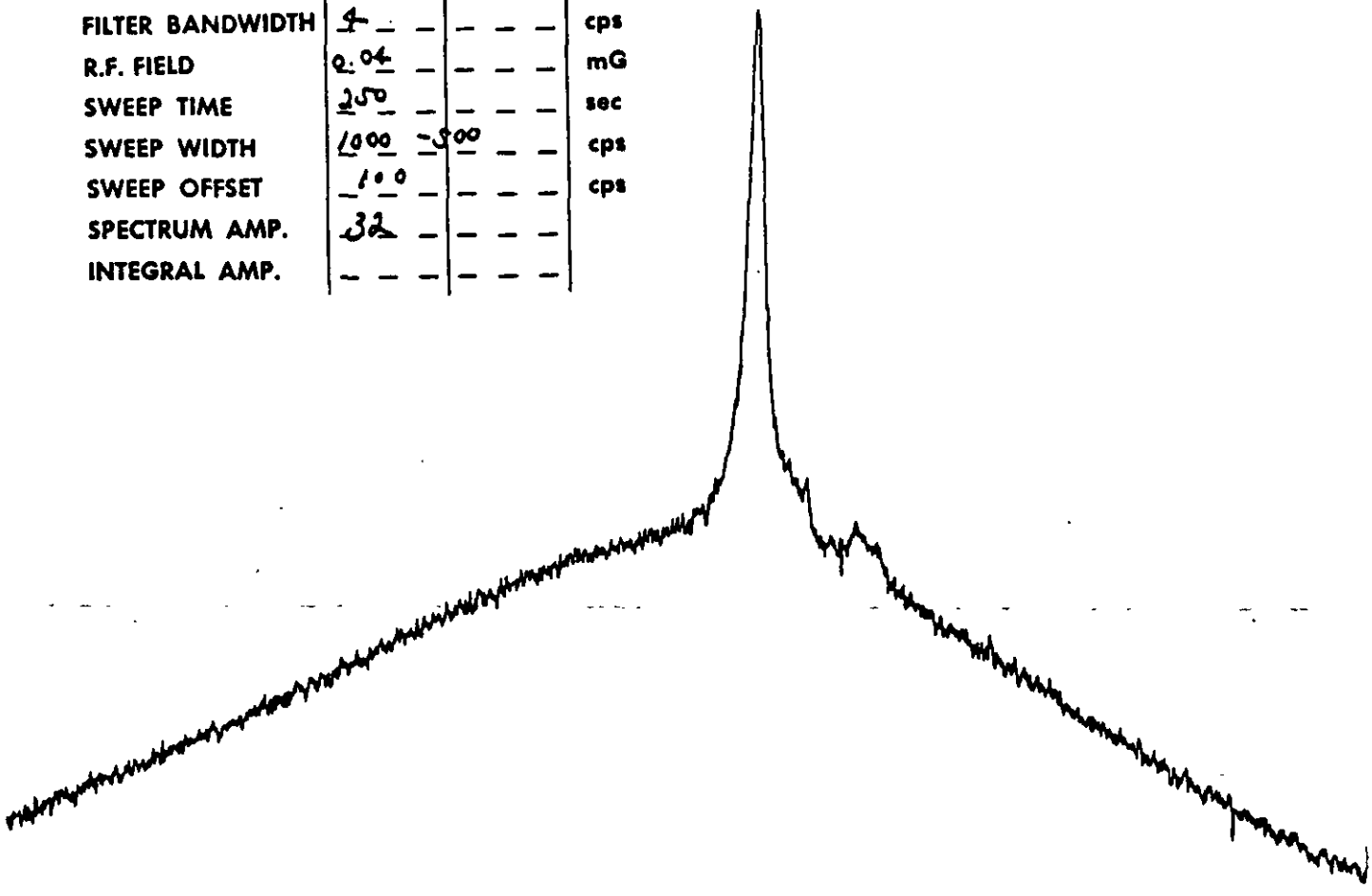

Figure 1. Portion of the NMR Spectrum for Cyclohexane at -20°C.

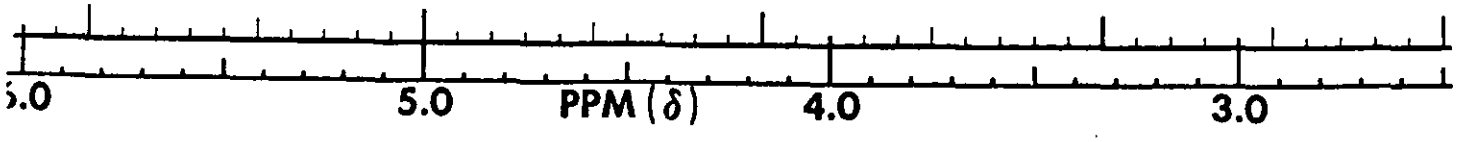

It was anticipated that the emphasis of this study would be on cyclohexanol because of its unusual phase relationships. Also the transition temperatures were more accessible than either cyclohexane or camphene. Once again we were besieged by the fact that the signal disappeared as the temperature was lowered. Figure 2 compares the spectra of cyclohexanol at three temperatures, +33°, +25° and +12°C. (The sample melts at 25°C.) The spectra are similar to those reported in the literature. Actually the spectrum for cyclohexanol shows three well separated peaks. The area under the peaks is in the ratio of 1:1:10 as would be expected. Only the largest peak is shown in Figure 2.

If one compares the thermal variation of the peaks of cyclohexane and cyclohexanol there is one obvious difference. The width of the cyclohexanol peak remains essentially constant as the temperature is lowered and there is no evidence af any superposition on a broad peak. The width of the line is an indication of the motional behavior of the molecule. Since the width does not change, the assumption is that the motion of the molecule in the solid state is very similar to that in the liquid state. This reasoning is consistent with the results from dielectric constant measurements. An examination of the smaller two peaks in the spectrum reveals that the OH peak does broaden out as the temperature decreases. It also shifts to a lower field. There is no shift in the other two peaks.

If the cold blast theory is valid, the resulting phase transformation would account for the loss of signal. However, the phase transformation is

unlikely because cyclohexanol is easily supercooled. The line width at +8°C aggrees favorably with the value estimated from the literature.

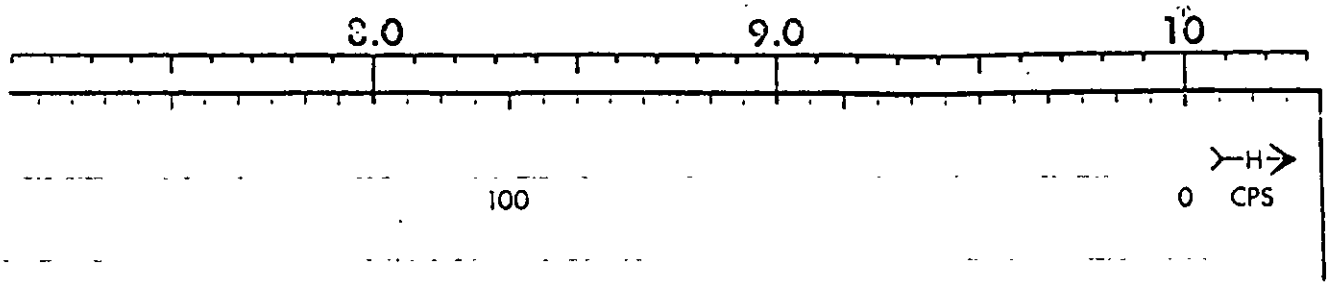

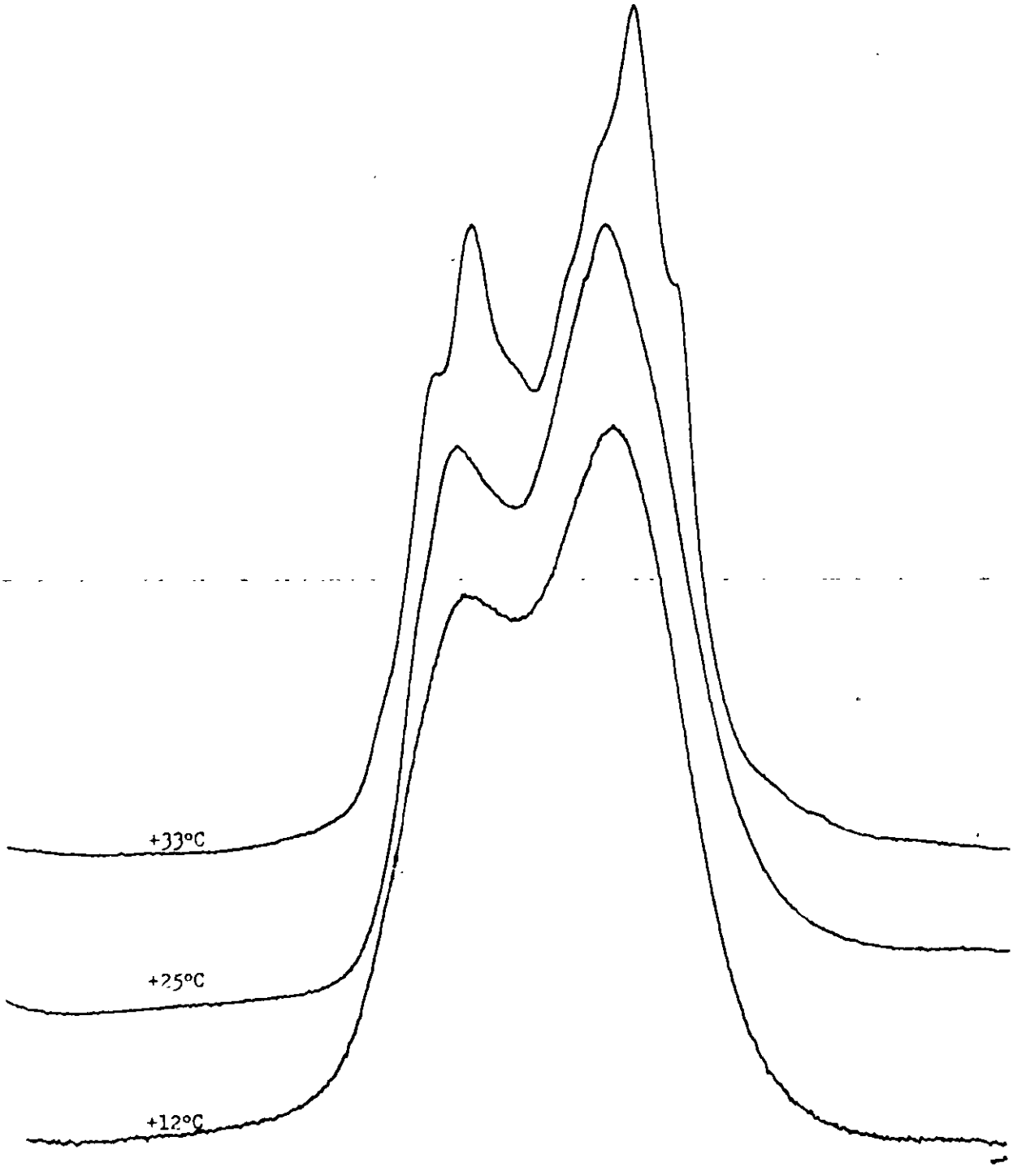

Figure 2. Temperature variation of NMR spectra of cyclohexene

Camphene behaved as would be predicted from x-ray and density measurements. Figure 3 shows the spectra at six temperatures. Although the amplitude of the peak did decrease with temperature the areas under the curve remained about the same. The broadening of the line is probably due to a hindering of the self diffusion process which was mentioned previously. Unfortunately, there is no data below -12°C. The limited data on line width are shown in Figure 4. There is a slight indication that the curve will become more horizontal at temperatures lower than -12°. If so, it may be true that the self diffusion sets in at about -20°C.

Unfortunately, the material described here as camphene is not pure camphene, as determined by integrating the NMR spectrum and also a gas chromatographic analysis. A sample of the material used in the x-ray, density and dielectric measurements was obtained and it has the same impurities so a comparison is legitimate.

The line widths were calculated by using the microcomparator to read the coordinates of the spectra which were on photographic negatives. The derivative of the lines were then computed. It was found that in the case of the well behaved curves for camphene the line width could be estimated directly from the curve.

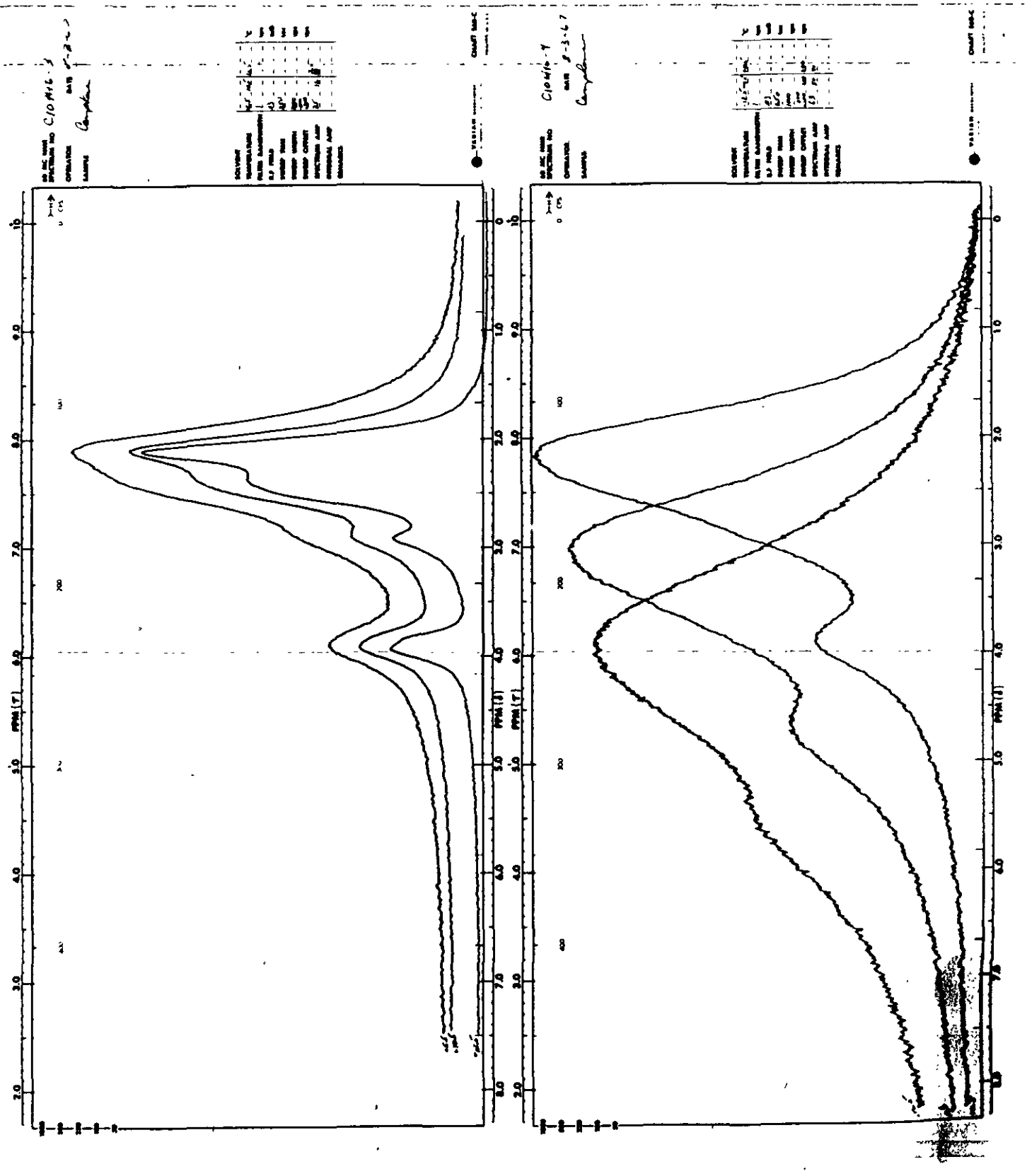

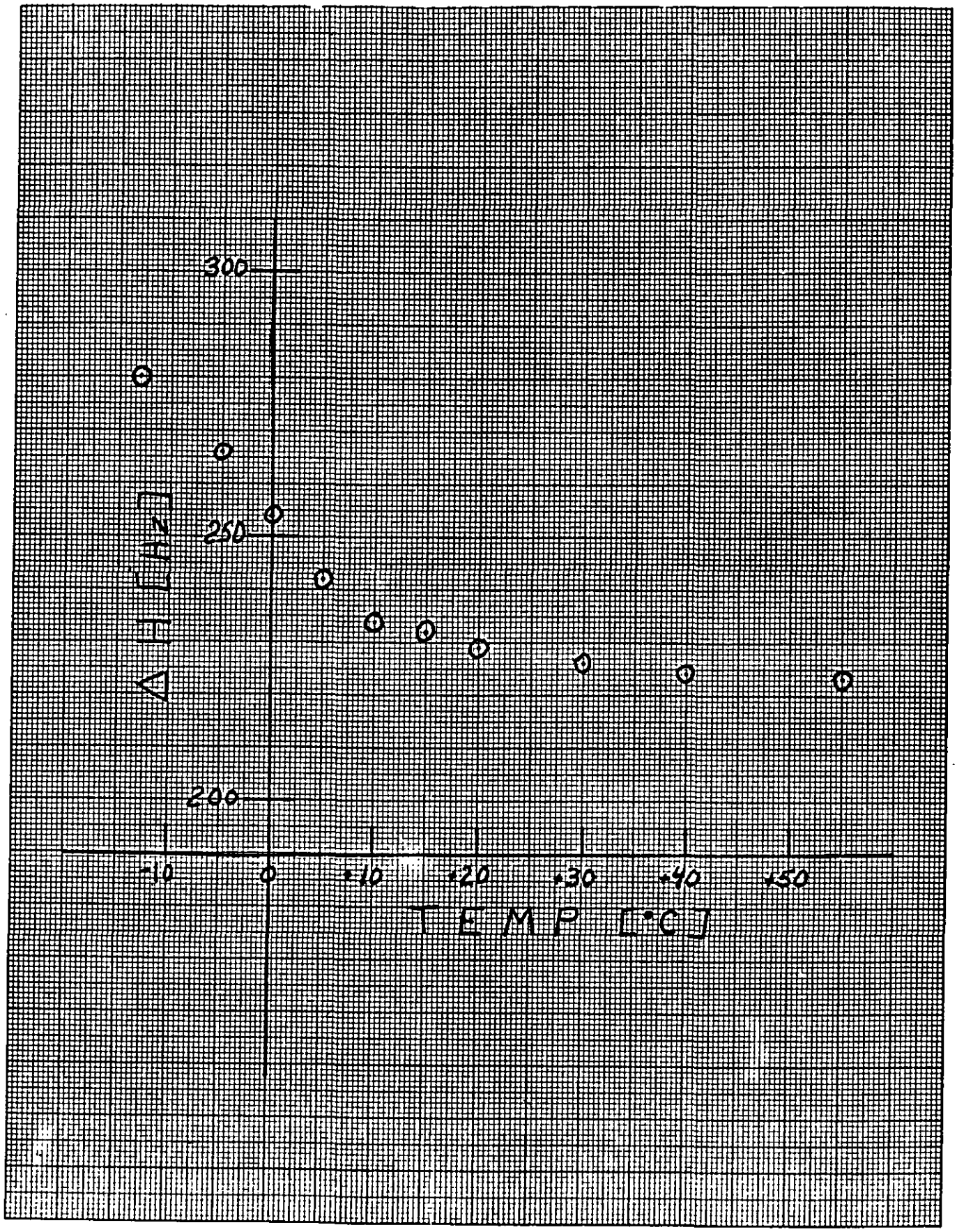

Figure 4. Line Width vs Temperature for Camphene

FUTURE WORK

One would have to conclude that the A-60A is not very well suited as a general tool to examine the motional behavior of the molecules in plastic solids. There are, however, certain specific problems that can be investigated. The superposition of the two peaks in the cyclohexane spectra, which commence at the melting point, may merit further investigation. Certainly an investigation of a pure sample of camphene would be of interest. The hindering of molecular motion by impurities is a study all in itself.

Although the high resolution NMR spectra are useful in investigating the molecular motion in plastic solids, it appears necessary that a dual purpose spectrometer (both high resolution and wide line) is required for a complete analysis. This would be especially true when the system is expanded to molecular motion of groups or segments on a polymer chain.

ACKNOWLEDGMENTS

I would like to thank the following persons who were most helpful:

Mr. L. Sell for his assistance in operating the spectrometer.

Dr. D. Johnson for his many discussions.

Dr. R. Holm and Mr. R. Helms for their work on the computer program for determining line widths from the spectra curves.

Mr. D. Wheeler (University of New Mexico, Dept. of Physics) for sharing his camphene sample.

BIBLIOGRAPHY

1. Andrew, E. R., J. Phys. Chem. Solids, 18, 9-16 (1961). "Nuclear magnetic resonance in solids containing small molecules."

2. Symposium on Plastic Crystals and Rotation in the Solid State, Oxford University, April, 1960. Proceedings published in J. Phys. Chem. Solids, 18, 1-90 (1961).

3. Smyth, C. P., Dielectric Behavior and Structure. McGraw-Hill, New York (1955).

4. Gutowsky, H. S., and Pake, G. E., J. Chem. Phys. 18, 162-70 (1950). "Structural investigations by means of nuclear magnetism. II. Hindered rotation in solids."

5. Green, J. R., and Scheie, C. E., J. Phys. Chem. Solids, 28, 383-94 (1967). "Ultrasonic investigation of solid dl-camphene, cyclohexane and cyclohexanol."

6. Iwayanagi, S. and Sakurai, I., J. Polymer Sci. PtC, Polymer Symp. no. 15, 29-53 (1966). "NMR Study of Molecular Motions in Some Crystalline Polymers."

7. Andrew, E. R., Nuclear Magnetic Resonance. Cambridge University Press (1956).

8. Kittel, C., Introduction to Solid State Physics. Wiley, New York (1966).

9. Pople, J. A., Schneider, W. G., and Bernstein, H. J., High-resolution Nuclear Magnetic Resonance. McGraw-Hill, New York (1959).

10. Parks, G. S., Huffman, H. M. and Thomas, J. B., J. Am. Chem. Soc. 52, 1032-41 (1930). "Thermal Data on Organic Compounds."

11. Timmermans, J., Les Constantes Physiques des Composes Organiques Cristalles. Masson, Paris (1953).

12. Kelley, K. K., J. Am. Chem. Soc., 73, 1400-6 (1929). "Cyclohexanol and the Third Law of Thermodynamics."

13. Andrew, E. R., and Eades, R. G., Proc. Roy. Soc. 216A, 398-412 (1953). "A nuclear magnetic resonance investigation of solid cyclohexane."

14. Born , M. and Huang, K., Dynamical Theory of Crystal Lattices. Oxford University Press, London (1956).

15. Wheeler, D. R., and Green, J. R., Unpublished report (1967). "An x-ray study of the plastic crystal modification of camphene."

16. Griffith, W. T., and Green, J. R., Unpublished report (1967). "Growth rates of phase transformations in solid cyclohexanol."

17. Averbuch, P., C. R. Acad. Sci. Paris 244, 3147-50 (1957). "Étude de la résonance paramagnétique nucléaire des protons dans le cyclohexanol solide en fonction de la température."

18. Suga, H. and Seki, S., Bull. Chem. Soc. Japan, 35, 1905-6 (1962). "High-resolution NMR spectra of crystalline cyclohexanol."